Time-dependent current-density-functional theory for the metallic response of solids

P. Romaniello and P. L. de Boeij*
Theoretical Chemistry, Materials Science Centre, Rijksuniversiteit Groningen, Nijenborgh 4, 9747 AG Groningen, The Netherlands
(Received 13 July 2004; revised manuscript received 19 January 2005; published 13 April 2005)

We extend the formulation of time-dependent current-density-functional theory for the linear response properties of dielectric and semi-metallic solids [Kootstra *et al.*, J. Chem. Phys. **112**, 6517 (2000)] to treat metals as well. To achieve this, the Kohn-Sham response functions have to include both interband and intraband transitions with an accurate treatment of the Fermi surface in the Brillouin-zone integrations. The intraband contributions in particular have to be evaluated using a wave-vector-dependent description. To test the method we calculate the optical properties of the two noble metals Cu and Ag. The dielectric and energy loss functions are compared with experiments and with the classical Drude theory. In general we find a good agreement with the experiments for the calculated results obtained within the adiabatic local density approximation. In order to describe the Drude-like absorption below the interband onset and the sharp plasma feature in silver exchange-correlation, effects beyond the adiabatic local density approximation are needed, which may be included in a natural way in the present current-density-functional approach.

DOI: 10.1103/PhysRevB.71.155108 PACS number(s): 71.45.Gm, 78.20.Ci

I. INTRODUCTION

In time-dependent density-functional theory (TDDFT), developed by Runge and Gross[1] starting from the original ground-state Hohenberg-Kohn formulation,[2,3] the exact dynamical response of a many-particle system to an external perturbing time-dependent scalar potential can be obtained using an effective one-particle description.[1,4–6] Many-particle effects enter in the time-dependent version of the so-called Kohn-Sham scheme[3] through the exchange-correlation contribution to the self-consistent and time-dependent effective scalar potential. Ghosh and Dhara[7,8] extended the Runge-Gross theorem[1] to many-particle systems in a general time-dependent electromagnetic field. In their description the electron current-density enters, replacing the electron density of ordinary TDDFT as the fundamental dynamical variable, with the vector potential instead of the scalar potential as its natural conjugate variable.[9] This time-dependent current-density functional approach (TDCDFT)[5,10,11] is particularly well-suited for the treatment of extended systems.[12,13] When such a system is perturbed by an external electric field, there will be a macroscopic response caused by charge accumulating at the outer surface that leads to a macroscopic screening field inside the bulk. The continuity relation implies that the density change at the surface of the system is accompanied by a current flowing through the interior with a nonzero average value for the current-density. When treating the response of a crystalline system by using periodic boundary conditions within TDDFT, the effect of this phenomenon called macroscopic polarization cannot be described using the periodic bulk density alone,[14] and one has to introduce additional dynamical variables to account for the surface charge, c.q. the macroscopic polarization[15] or, equivalently, the macroscopic induced field.[16] In the TDCDFT approach the information on the surface charge is already contained in a natural way in the periodic current-density. For the longitudinal response of isotropic systems, some of the difficulties can be circumvented by relating the long-wavelength limit of the density-density response to the longitudinal current-current response.[17–20] The (current-)density functional approach yields reasonable results for the dielectric constants and optical dielectric functions of various isotropic semiconductors and insulators when it is used within the adiabatic local density approximation (ALDA) for the exchange-correlation field,[12,13,21–26] but more advanced schemes involving long-range kernels,[27–32] or equivalently (semi)-local current functionals,[11,33,34] are needed to account for excitonic effects in these systems. For anisotropic system and when calculating transverse response at $q>0$ we have to use the TDCDFT approach, which can be applied to treat the optical properties of metals as well. Here, however, one should not only consider the interband contribution, involving transitions from (partially) occupied to (partially) unoccupied bands as in nonmetals, but also the intraband contribution due to transitions within the same band, more specifically, from just below the Fermi level to just above this level. The latter processes are responsible for the collective plasmon response typical for simple metallic systems.[17] For the noble metals like Ag and Cu the interplay between inter- and intraband processes involving *d*-electrons leads to a strong redshift of the Drude-like plasmon resonance.[35–39]

In this paper we give a general description of the response of a metallic system to an external electromagnetic field within the current-density functional scheme.[12,13] To achieve this we consider a general q- and ω-dependent perturbation,

$$\delta\hat{h}(\mathbf{r},t) = \delta\hat{h}_{\mathbf{q}}(\mathbf{r},\omega)e^{i(\mathbf{q}\cdot\mathbf{r}-\omega t)}, \tag{1}$$

where we choose $\delta\hat{h}_{-\mathbf{q}}(\mathbf{r},-\omega) = \delta\hat{h}^{\dagger}_{\mathbf{q}}(\mathbf{r},\omega)$ to ensure a real perturbation with $\delta\hat{h}_{\mathbf{q}}(\mathbf{r},\omega)$ lattice periodic. We derive the linear response of the system for vanishing q but finite ω. This is the regime describing optical properties. To evaluate the response in this limit three steps are essential. First we show that the inter- and intraband processes behave differently for small q. Then we show that we can still use the microscopic Coulomb gauge[12] to separate microscopic and macroscopic

contributions to the effective scalar and vector potentials. Finally, we consider the self-consistent-field equations and show that inter- and intraband contributions to the response decouple in the optical limit when we make use of the adiabatic local density approximation. Here we outline the derivation, which can be found in full detail in the next section. We start by expressing the induced density and current-density using the q-dependent Kohn-Sham response functions. These take the following general form,

$$\chi_{ab\mathbf{q}}(\mathbf{r},\mathbf{r}',\omega) = \frac{1}{N_k}\sum_{\mathbf{k}}\sum_{i,a} \times \frac{(f_{i\mathbf{k}}-f_{a\mathbf{k}+\mathbf{q}})}{1+\delta_{i,a}} \frac{[\psi^*_{i\mathbf{k}}(\mathbf{r})\hat{a}\psi_{a\mathbf{k}+\mathbf{q}}(\mathbf{r})][\psi^*_{a\mathbf{k}+\mathbf{q}}(\mathbf{r}')\hat{b}\psi_{i\mathbf{k}}(\mathbf{r}')]}{\epsilon_{i\mathbf{k}}-\epsilon_{a\mathbf{k}+\mathbf{q}}+\omega+i\eta} + \text{c.c.}(-\mathbf{q},-\omega),$$

where $\hat{a}$ and $\hat{b}$ refer to the operators $\hat{\rho}=1$ or $\hat{\mathbf{j}}=-i(\nabla-\nabla^{\dagger})/2$, and the summation is over the (partially) occupied bands, i, and (partially) unoccupied bands, a. Only ground state orbitals $\psi_{n\mathbf{k}}$, orbital energies $\epsilon_{n\mathbf{k}}$, and occupation numbers $f_{n\mathbf{k}}$ enter in this expression, which takes into account the conservation of the crystal momentum. The Bloch functions are normalized on the Wigner-Seitz cell V_{WS}, and the number of $\mathbf{k}$ points in the summation is $N_k=V_{BvK}/V_{WS}$, in which V_{BvK} is the volume of the Born–von Kármán cell. The intraband (interband) contribution to the response functions is given by the terms with $a=i$ ($a\neq i$) in the summation over i and a. In the intraband case the factor $1/(1+\delta_{i,a})$ corrects for the double counting. Analysis of the q dependence at finite ω indicates that the intraband contributions vanish in the limit $q\to 0$ except for $\chi_{\mathbf{jjq}}(\mathbf{r},\mathbf{r}',\omega)$. By considering the reverse order of limits, i.e., by evaluating the limit $\omega\to 0$ before taking $q\to 0$, we retrieve the conductivity sum rule which allows us to relate the diamagnetic and paramagnetic components of the current-density. Identifying the various contributions to the response functions makes it possible to separate the inter- and intraband contributions to the induced density and current-density,

$$\delta\rho(\mathbf{r},\omega)=\delta\rho^{inter}(\mathbf{r},\omega)+\delta\rho^{intra}(\mathbf{r},\omega),$$

$$\delta\mathbf{j}(\mathbf{r},\omega)=\delta\mathbf{j}^{inter}(\mathbf{r},\omega)+\delta\mathbf{j}^{intra}(\mathbf{r},\omega). \quad (2)$$

The equations for the interband contribution to the density and current-density become identical to the original description of Kootstra *et al.*[12,13] in the limit of q to zero. The description of the intraband contribution follows along the same lines as for the interband case. In the description of Kootstra *et al.* it is proven to be essential to choose the gauge such that the macroscopic component of the induced electric field that is due to the induced density and current-density is completely described using the vector potential. The scalar potential is thus purely microscopic. One can then obtain the response to a fixed macroscopic field instead of to an external field and thus treat the macroscopic optical response exactly.[12] This still holds in our q-dependent description, where it turns out that the density and current-density have the same q dependence as the perturbing field. We can then define the macroscopic induced density as

$$\delta\rho_{mac}(\mathbf{r},\omega)=e^{i\mathbf{q}\cdot\mathbf{r}}\frac{1}{V}\int_V e^{-i\mathbf{q}\cdot\mathbf{r}}\delta\rho(\mathbf{r},\omega)\,d\mathbf{r}, \quad (3)$$

where V is the unit cell, and similarly we can define the macroscopic current-density. A careful analysis of the q dependence at small q, but finite ω, reveals that we can include in the microscopic scalar potential the contribution due to the intraband part of the microscopic induced density,

$$\delta\rho^{intra}_{mic}(\mathbf{r},\omega)=\delta\rho^{intra}(\mathbf{r},\omega)-\delta\rho^{intra}_{mac}(\mathbf{r},\omega),$$

where $\delta\rho^{intra}_{mac}(\mathbf{r},\omega)$ is the macroscopic part of the intraband induced density. The other contributions that lead to a macroscopic field have to be included in the vector potential. Intraband contributions to both the microscopic scalar potential and macroscopic vector potential are now identified. The former vanishes in the limit of q to zero, and the latter is to be included in the definition of the fixed macroscopic field. Like in the description of Kootstra *et al.* we can neglect the very small microscopic magnetic contribution to the self-consistent field, which is due to the transverse current. Together with the classical potentials, we also have to consider the exchange-correlation contribution to the self-consistent field. We find that in the optical limit only the exchange-correlation contribution of the interband part of the induced density needs to be included in the microscopic scalar potential to arrive at the same adiabatic local density approximation (ALDA) used in the ordinary TDDFT approach. At the same time no exchange-correlation contributions to the macroscopic vector potential remain. In this work we neglect possible additional contributions from the induced current.[33] The microscopic effective scalar potential is thus completely determined by the microscopic interband induced density. Therefore we can obtain the response in the optical limit by first solving the equations for the interband part of the density and by subsequently obtaining the intraband part. We show that, whereas the interband density needs a self-consistent solution, in the second stage the intraband density and the current-density do not need to be calculated self-consistently. It follows that the intraband current can be obtained completely independent from the interband density and current-density and *vice versa*. Note, however, that for finite q and for exchange-correlation approximations that go beyond the ALDA the sets of equations are essentially coupled.

The remainder of the paper is organized as follows. The main aspects of the implementation are given in a separate section. This implementation is based on the description of Kootstra *et al.*[12] for the q-independent nonmetallic case. Here we focus on the specific case of metals and refer the reader to Ref. 12 for the general framework used. Finally, we report our results for the dielectric and energy loss functions for the crystals of Cu and Ag and compare them with the best available experimental data.[35–39]

II. THEORY

We treat the dynamic linear response of a metallic crystal to a perturbation described by both scalar and vector potentials within the time-dependent current-density-functional theory (TDCDFT).[5,7,8,10,11] In the effective one-electron scheme of Kohn-Sham,[3] non-interacting particles moving in a time-dependent effective electromagnetic field are described by Bloch functions that are solutions of the following equation,

$$i\frac{\partial}{\partial t}\psi_{n\mathbf{k}}(\mathbf{r},t) = \left[\frac{1}{2}\left(\hat{\mathbf{p}} + \frac{1}{c}\delta\mathbf{a}_{eff}(\mathbf{r},t)\right)^2 + v_{eff,0}(\mathbf{r}) + \delta v_{eff}(\mathbf{r},t)\right]\psi_{n\mathbf{k}}(\mathbf{r},t). \quad (4)$$

Here $v_{eff,0}(\mathbf{r})$ is the effective scalar potential giving the initial density which we choose to be the ground state density. It is, therefore, uniquely determined by the Hohenberg-Kohn theorem.[2] The time-dependent potentials $\delta v_{eff}(\mathbf{r},t)$ and $\delta\mathbf{a}_{eff}(\mathbf{r},t)$ produce the exact time-dependent density and current-density for the chosen initial state,

$$\rho(\mathbf{r},t) = \sum_{n,\mathbf{k}} f_{n\mathbf{k}}\psi^*_{n\mathbf{k}}(\mathbf{r},t)\psi_{n\mathbf{k}}(\mathbf{r},t), \quad (5)$$

where $f_{n\mathbf{k}}$ are the occupation numbers, and

$$\mathbf{j}(\mathbf{r},t) = \sum_{n,\mathbf{k}} f_{n\mathbf{k}}\psi^*_{n\mathbf{k}}(\mathbf{r},t)\hat{\mathbf{j}}\psi_{n\mathbf{k}}(\mathbf{r},t) + \frac{1}{c}\rho(\mathbf{r},t)\delta\mathbf{a}_{eff}(\mathbf{r},t). \quad (6)$$

In Eq. (6) the first term is the paramagnetic component of the current-density, in which the paramagnetic current operator $\hat{\mathbf{j}}$ is defined as $-i(\nabla-\nabla^\dagger)/2$ where the dagger indicates that terms to the left have to be differentiated. The second term is the diamagnetic component. Since the initial state is the ground state, the occupation numbers $f_{n\mathbf{k}}$ are given by the Fermi-Dirac distribution function $f_{n\mathbf{k}}=f(\epsilon_{n\mathbf{k}})=2$ for $\epsilon_{n\mathbf{k}}\leqslant\epsilon_F$ and 0 otherwise, with $\epsilon_{n\mathbf{k}}$ the ground state orbital energies and ϵ_F the Fermi level. The time-dependent potentials are uniquely determined up to an arbitrary gauge due to the Ghosh-Dhara theorem.[7,8] Both the density and the current-density are gauge invariant. The first-order perturbation of the ground state is governed by the perturbation Hamiltonian $\delta\hat{h}_{eff}$ containing all terms linear in the field,

$$\delta\hat{h}_{eff}(\mathbf{r},t) = \frac{1}{2c}[\hat{\mathbf{p}}\cdot\delta\mathbf{a}_{eff}(\mathbf{r},t) + \delta\mathbf{a}_{eff}(\mathbf{r},t)\cdot\hat{\mathbf{p}}] + \delta v_{eff}(\mathbf{r},t). \quad (7)$$

We choose the gauge to be the microscopic Coulomb gauge of Kootstra *et al.*[12] in which the effective scalar and vector potentials are given by

$$\delta v_{eff}(\mathbf{r},t) = \delta v_{H,mic}(\mathbf{r},t) + \delta v_{xc}(\mathbf{r},t), \quad (8)$$

$$\delta\mathbf{a}_{eff}(\mathbf{r},t) = -c\int^t \mathbf{E}_{mac}(\mathbf{r},t')dt' + \delta\mathbf{a}_{xc}(\mathbf{r},t), \quad (9)$$

where $\delta v_{H,mic}(\mathbf{r},t)$ and $\delta v_{xc}(\mathbf{r},t)$ are the microscopic component of the Hartree and exchange-correlation potentials, respectively, and $\mathbf{E}_{mac}(\mathbf{r},t')$ is the fixed macroscopic electric field, comprising both the external and the induced macroscopic components. The latter accounts for the long-range contribution of the Hartree potential, as well as for the properly retarded macroscopic contribution of the induced transverse current-density. We can neglect the microscopic part of the induced vector potential consistent with the Breit approximation used in the ground state calculation.[12,13,40,41] As described in the previous section we consider the macroscopic exchange-correlation contributions to be included in $\delta\mathbf{a}_{eff}$ via $\delta\mathbf{a}_{xc}$. We work in the frequency domain for simplicity,

$$\delta\mathbf{a}_{eff}(\mathbf{r},t) = \int e^{-i\omega t}\delta\mathbf{a}_{eff}(\mathbf{r},\omega)\,d\omega, \quad (10)$$

and consider a general perturbation characterized by wave vector $\mathbf{q}$ and frequency ω,

$$\delta\mathbf{a}_{eff}(\mathbf{r},\omega) = e^{i\mathbf{q}\cdot\mathbf{r}}\delta\mathbf{a}_{\mathbf{q},eff}(\mathbf{r},\omega), \quad (11)$$

in which $\delta\mathbf{a}_{\mathbf{q},eff}(\mathbf{r},\omega)$ is lattice periodic,

$$\delta\mathbf{a}_{\mathbf{q},eff}(\mathbf{r}+\mathbf{R},\omega) = \delta\mathbf{a}_{\mathbf{q},eff}(\mathbf{r},\omega), \quad (12)$$

for any Bravais lattice vector $\mathbf{R}$. Since the field given by Eqs. (10) and (11) is real we have

$$\delta\mathbf{a}_{\mathbf{q},eff}(\mathbf{r},\omega) = \delta\mathbf{a}^*_{-\mathbf{q},eff}(\mathbf{r},-\omega). \quad (13)$$

Similar expressions are assumed for the scalar potential $\delta v_{eff}(\mathbf{r},t)$. In the remainder we will only consider plane-wave vector potentials, i.e., $\delta\mathbf{a}_{\mathbf{q},eff}(\mathbf{r},\omega)=\delta\mathbf{a}_{\mathbf{q},eff}(\omega)$, unless stated otherwise.

A. Induced density

Using the Bloch theorem, we show in the Appendix that in the linear regime the induced density can be written as

$$\delta\rho(\mathbf{r},\omega) = e^{i\mathbf{q}\cdot\mathbf{r}}\delta\rho_{\mathbf{q}}(\mathbf{r},\omega), \quad (14)$$

where $\delta\rho_{\mathbf{q}}(\mathbf{r},\omega)$ is lattice periodic, $\delta\rho_{\mathbf{q}}(\mathbf{r}+\mathbf{R},\omega)=\delta\rho_{\mathbf{q}}(\mathbf{r},\omega)$, given by

$$\delta\rho_{\mathbf{q}}(\mathbf{r},\omega) = \frac{1}{N_k}\sum_{\mathbf{k},\mathbf{k}'}\delta_{\mathbf{k}',\mathbf{k}+\mathbf{q}}\sum_{i,a}\frac{(f_{i\mathbf{k}}-f_{a\mathbf{k}'})}{1+\delta_{ia}} \times\frac{\psi^*_{i\mathbf{k}}(\mathbf{r})e^{-i\mathbf{q}\cdot\mathbf{r}}\psi_{a\mathbf{k}'}(\mathbf{r})\langle\psi_{a\mathbf{k}'}|\delta\hat{h}(\mathbf{q},\omega)|\psi_{i\mathbf{k}}\rangle}{\epsilon_{i\mathbf{k}}-\epsilon_{a\mathbf{k}'}+\omega+i\eta} + \frac{1}{N_k}\sum_{\mathbf{k},\mathbf{k}'}\delta_{\mathbf{k}',\mathbf{k}-\mathbf{q}}\sum_{i,a}\frac{(f_{a\mathbf{k}'}-f_{i\mathbf{k}})}{1+\delta_{ia}} \times\frac{\psi^*_{a\mathbf{k}'}(\mathbf{r})e^{-i\mathbf{q}\cdot\mathbf{r}}\psi_{i\mathbf{k}}(\mathbf{r})\langle\psi_{i\mathbf{k}}|\delta\hat{h}(\mathbf{q},\omega)|\psi_{a\mathbf{k}'}\rangle}{\epsilon_{a\mathbf{k}'}-\epsilon_{i\mathbf{k}}+\omega+i\eta}, \quad (15)$$

in which we introduced the short-hand notation

$$\delta\hat{h}(\mathbf{q},\omega) = \frac{-i}{2c}(e^{i\mathbf{q}\cdot\mathbf{r}}\nabla - \nabla^{\dagger}e^{i\mathbf{q}\cdot\mathbf{r}})\cdot\delta\mathbf{a}_{\mathbf{q},eff}(\omega) + e^{i\mathbf{q}\cdot\mathbf{r}}\delta v_{\mathbf{q},eff}(\mathbf{r},\omega). \tag{16}$$

For future reference we define the additional short-hand notations, $\hat{\mathbf{j}}_{\mathbf{q}} = -i(e^{-i\mathbf{q}\cdot\mathbf{r}}\boldsymbol{\nabla} - \boldsymbol{\nabla}^{\dagger}e^{-i\mathbf{q}\cdot\mathbf{r}})/2$, and $\hat{\rho}_{\mathbf{q}} = e^{-i\mathbf{q}\cdot\mathbf{r}}$. The lattice-periodicity of $\delta\rho_{\mathbf{q}}(\mathbf{r},\omega)$ allows us to define the macroscopic induced density as

$$\delta\rho_{mac}(\mathbf{r},\omega) = e^{i\mathbf{q}\cdot\mathbf{r}}\frac{1}{V}\int_{V}\delta\rho_{\mathbf{q}}(\mathbf{r},\omega)\,d\mathbf{r}, \tag{17}$$

where the average is taken over the unit cell. In Eq. (15) the second term is the complex conjugate of the first one at $-\mathbf{q}$ and $-\omega$, so the induced density $\delta\rho(\mathbf{r},t)$ is real-valued, since $\delta\rho_{\mathbf{q}}(\mathbf{r},\omega) = \delta\rho^{*}_{-\mathbf{q}}(\mathbf{r},-\omega)$. Using time-reversal symmetry (see the Appendix) we can write Eq. (15) as

$$\begin{aligned}\delta\rho_{\mathbf{q}}(\mathbf{r},\omega) = \frac{1}{N_k}\sum_{\mathbf{k},\mathbf{k}'}\sum_{i,a} w_{i\mathbf{k}a\mathbf{k}',+}(\omega)\{&\delta_{\mathbf{k}',\mathbf{k}+\mathbf{q}}(\psi^{*}_{i\mathbf{k}}\hat{\rho}_{\mathbf{q}}\psi_{a\mathbf{k}'})\\ &\times\langle\psi_{a\mathbf{k}'}|\delta\hat{h}_e(\mathbf{q},\omega)|\psi_{i\mathbf{k}}\rangle + \delta_{\mathbf{k}',\mathbf{k}-\mathbf{q}}(\psi^{*}_{a\mathbf{k}'}\hat{\rho}_{\mathbf{q}}\psi_{i\mathbf{k}})\\ &\times\langle\psi_{i\mathbf{k}}|\delta\hat{h}_e(\mathbf{q},\omega)|\psi_{a\mathbf{k}'}\rangle\} + \frac{1}{N_k}\sum_{\mathbf{k},\mathbf{k}'}\sum_{i,a} w_{i\mathbf{k}a\mathbf{k}',-}(\omega)\\ &\times\{\delta_{\mathbf{k}',\mathbf{k}+\mathbf{q}}(\psi^{*}_{i\mathbf{k}}\hat{\rho}_{\mathbf{q}}\psi_{a\mathbf{k}'})\langle\psi_{a\mathbf{k}'}|\delta\hat{h}_o(\mathbf{q},\omega)|\psi_{i\mathbf{k}}\rangle\\ &- \delta_{\mathbf{k}',\mathbf{k}-\mathbf{q}}(\psi^{*}_{a\mathbf{k}'}\hat{\rho}_{\mathbf{q}}\psi_{i\mathbf{k}})\langle\psi_{i\mathbf{k}}|\delta\hat{h}_o(\mathbf{q},\omega)|\psi_{a\mathbf{k}'}\rangle\}.\end{aligned} \tag{18}$$

Here the $\mathbf{r}$ dependence of the Bloch orbitals has been implied and we have defined the "even" and "odd" components of the interaction Hamiltonian according to

$$\delta\hat{h}_e(\mathbf{q},\omega) = \frac{1}{2}[\delta\hat{h}(\mathbf{q},\omega) + \delta\hat{h}^{*}(-\mathbf{q},-\omega)] = \hat{\rho}_{-\mathbf{q}}\delta v_{\mathbf{q},eff}(\mathbf{r},\omega), \tag{19}$$

$$\delta\hat{h}_o(\mathbf{q},\omega) = \frac{1}{2}[\delta\hat{h}(\mathbf{q},\omega) - \delta\hat{h}^{*}(-\mathbf{q},-\omega)] = \frac{1}{c}\hat{\mathbf{j}}_{-\mathbf{q}}\cdot\delta\mathbf{a}_{\mathbf{q},eff}(\omega), \tag{20}$$

where $\delta\hat{h}^{*}(-\mathbf{q},-\omega)$ is the complex conjugate (not the Hermitian adjoint) of $\delta\hat{h}(\mathbf{q},\omega)$ at negative $\mathbf{q}$ and ω. The energy denominators and the occupation numbers in Eq. (15) are contained in the frequency-dependent weights,

$$w_{i\mathbf{k}a\mathbf{k}',\pm}(\omega) = \frac{f_{i\mathbf{k}} - f_{a\mathbf{k}'}}{2(1+\delta_{ia})}\times\left\{\frac{1}{\epsilon_{i\mathbf{k}} - \epsilon_{a\mathbf{k}'} + \omega + i\eta} \pm \frac{1}{\epsilon_{i\mathbf{k}} - \epsilon_{a\mathbf{k}'} - \omega - i\eta}\right\}. \tag{21}$$

Simple algebra shows that $w_{i\mathbf{k}a\mathbf{k}',+}(\omega)$ and $w_{i\mathbf{k}a\mathbf{k}',-}(\omega)$ are related,

$$w_{i\mathbf{k}a\mathbf{k}',-}(\omega) = -\frac{\epsilon_{i\mathbf{k}} - \epsilon_{a\mathbf{k}'}}{\omega}\{w_{i\mathbf{k}a\mathbf{k}',+}(\omega) - w_{i\mathbf{k}a\mathbf{k}',+}(0)\}, \tag{22}$$

$$w_{i\mathbf{k}a\mathbf{k}',+}(\omega) = -\frac{\epsilon_{i\mathbf{k}} - \epsilon_{a\mathbf{k}'}}{\omega}w_{i\mathbf{k}a\mathbf{k}',-}(\omega). \tag{23}$$

B. Induced current-density

For the induced current-density we can derive expressions along the same lines used for the induced density. The paramagnetic component of the induced current-density can be obtained as

$$\delta\mathbf{j}_p(\mathbf{r},\omega) = e^{i\mathbf{q}\cdot\mathbf{r}}\delta\mathbf{j}_{p\mathbf{q}}(\mathbf{r},\omega), \tag{24}$$

where $\delta\mathbf{j}_{p\mathbf{q}}(\mathbf{r},\omega)$ is lattice periodic as well, and follows from

$$\begin{aligned}\delta\mathbf{j}_{p\mathbf{q}}(\mathbf{r},\omega) = \frac{1}{N_k}\sum_{\mathbf{k},\mathbf{k}'}\delta_{\mathbf{k}',\mathbf{k}+\mathbf{q}}\sum_{i,a}\frac{(f_{i\mathbf{k}} - f_{a\mathbf{k}'})}{1+\delta_{ia}}&\\ \times\frac{\psi^{*}_{i\mathbf{k}}\hat{\mathbf{j}}_{\mathbf{q}}\psi_{a\mathbf{k}'}\langle\psi_{a\mathbf{k}'}|\delta\hat{h}(\mathbf{q},\omega)|\psi_{i\mathbf{k}}\rangle}{\epsilon_{i\mathbf{k}} - \epsilon_{a\mathbf{k}'} + \omega + i\eta}&\\ + \frac{1}{N_k}\sum_{\mathbf{k},\mathbf{k}'}\delta_{\mathbf{k}',\mathbf{k}-\mathbf{q}}\sum_{i,a}&\\ \times\frac{(f_{a\mathbf{k}'} - f_{i\mathbf{k}})}{1+\delta_{ia}}\frac{\psi^{*}_{a\mathbf{k}'}\hat{\mathbf{j}}_{\mathbf{q}}\psi_{i\mathbf{k}}\langle\psi_{i\mathbf{k}}|\delta\hat{h}(\mathbf{q},\omega)|\psi_{a\mathbf{k}'}\rangle}{\epsilon_{a\mathbf{k}'} - \epsilon_{i\mathbf{k}} + \omega + i\eta}.&\end{aligned} \tag{25}$$

Here the second term is the complex conjugate of the first term, but at the negative $\mathbf{q}$ and negative frequency. In the linear regime the diamagnetic contribution is given by

$$\delta\mathbf{j}_d(\mathbf{r},\omega) = e^{i\mathbf{q}\cdot\mathbf{r}}\delta\mathbf{j}_{d\mathbf{q}}(\mathbf{r},\omega), \tag{26}$$

where

$$\delta\mathbf{j}_{d\mathbf{q}}(\mathbf{r},\omega) = \frac{1}{c}\rho_0(\mathbf{r})\,\delta\mathbf{a}_{\mathbf{q},eff}(\omega), \tag{27}$$

with $\rho_0(\mathbf{r})$ real and lattice periodic. As a result one finds also for the induced current-density the relation $\delta\mathbf{j}_{\mathbf{q}}(\mathbf{r},\omega) = \delta\mathbf{j}_{p\mathbf{q}}(\mathbf{r},\omega) + \delta\mathbf{j}_{d\mathbf{q}}(\mathbf{r},\omega) = \delta\mathbf{j}^{*}_{-\mathbf{q}}(\mathbf{r},-\omega)$ and thus a real-valued current-density $\delta\mathbf{j}(\mathbf{r},t)$. Using again the time-reversal symmetry the induced paramagnetic current-density can be written in a way very similar to Eq. (18),

$$\begin{aligned}\delta\mathbf{j}_{p\mathbf{q}}(\mathbf{r},\omega) = \frac{1}{N_k}\sum_{\mathbf{k},\mathbf{k}'}\sum_{i,a} w_{i\mathbf{k}a\mathbf{k}',+}(\omega)\{&\delta_{\mathbf{k}',\mathbf{k}+\mathbf{q}}(\psi^{*}_{i\mathbf{k}}\hat{\mathbf{j}}_{\mathbf{q}}\psi_{a\mathbf{k}'})\\ &\times\langle\psi_{a\mathbf{k}'}|\delta\hat{h}_o(\mathbf{q},\omega)|\psi_{i\mathbf{k}}\rangle + \delta_{\mathbf{k}',\mathbf{k}-\mathbf{q}}(\psi^{*}_{a\mathbf{k}'}\hat{\mathbf{j}}_{\mathbf{q}}\psi_{i\mathbf{k}})\\ &\times\langle\psi_{i\mathbf{k}}|\delta\hat{h}_o(\mathbf{q},\omega)|\psi_{a\mathbf{k}'}\rangle)\} + \frac{1}{N_k}\sum_{\mathbf{k},\mathbf{k}'}\sum_{i,a} w_{i\mathbf{k}a\mathbf{k}',-}(\omega)\\ &\times\{\delta_{\mathbf{k}',\mathbf{k}+\mathbf{q}}(\psi^{*}_{i\mathbf{k}}\hat{\mathbf{j}}_{\mathbf{q}}\psi_{a\mathbf{k}'})\langle\psi_{a\mathbf{k}'}|\delta\hat{h}_e(\mathbf{q},\omega)|\psi_{i\mathbf{k}}\rangle)\end{aligned}$$

$$- \delta_{\mathbf{k}',\mathbf{k}-\mathbf{q}}(\psi^*_{a\mathbf{k}'}\hat{\mathbf{j}}_{\mathbf{q}}\psi_{i\mathbf{k}})\langle\psi_{i\mathbf{k}}|\delta\hat{h}_e(\mathbf{q},\omega)|\psi_{a\mathbf{k}'}\rangle)\}, \tag{28}$$

where the weights are given by Eq. (21). Note that here the "even" and "odd" components of the perturbation, defined in Eqs. (19) and (20), have changed positions with respect to Eq. (18).

For the implementation it turns out to be convenient to relate the diamagnetic component of the induced current-density to the paramagnetic one, and treat both contributions on an equal footing. Before doing this we want to refer to the case of a homogeneous electron gas perturbed by a monochromatic field $\delta\mathbf{a}(\mathbf{r},\omega)$.[17] Indeed the induced total current-density is then given by

$$\delta\mathbf{j}(\mathbf{r},\omega) = \frac{1}{c}\int \chi_{\mathbf{jj}}(\mathbf{r},\mathbf{r}',\omega)\,\delta\mathbf{a}(\mathbf{r}',\omega)\,d\mathbf{r}' + \frac{1}{c}\rho_0(\mathbf{r})\,\delta\mathbf{a}(\mathbf{r},\omega), \tag{29}$$

where the exact current-current response function $\chi_{\mathbf{jj}}(\mathbf{r},\mathbf{r}',\omega)$ only depends on the distance $|\mathbf{r}-\mathbf{r}'|$. Its Fourier transform can be expressed in the following way,

$$\chi_{\mathbf{jj},\mu\nu}(\mathbf{q},\omega) = \chi_L(q,\omega)\frac{q_\mu q_\nu}{q^2} + \chi_T(q,\omega)\left(\delta_{\mu\nu} - \frac{q_\mu q_\nu}{q^2}\right), \tag{30}$$

with the longitudinal $\chi_L(q,\omega)$ and the transverse component $\chi_T(q,\omega)$ satisfying[17]

$$\lim_{q\to 0}\chi_T(q,\omega=0) = -\rho_0, \tag{31}$$

$$\chi_L(q,\omega=0) = -\rho_0. \tag{32}$$

For the value of $\chi_T(q,\omega=0)$ at finite q the corrections to this limit are of order q^2. In real space we can therefore write

$$\chi_{\mathbf{jj}}(\mathbf{r},\mathbf{r}',0) = -\rho_0\delta(\mathbf{r}-\mathbf{r}') + \Delta\chi_T(\mathbf{r},\mathbf{r}',0), \tag{33}$$

where $\Delta\chi_T(\mathbf{r},\mathbf{r}',0)$ is purely transverse, and hence responsible for the weak diamagnetism first calculated by Landau. Here we deal with two limits, $\lim \mathbf{q}\to 0$ and $\lim \omega\to 0$. The value of $\chi_T(q,\omega)$ depends on the order in which one takes the limits, since it is nonanalytic in the point (0,0) in the q-ω plane. In order to relate the diamagnetic and the paramagnetic contributions to the current-current response function, one has to consider first the limit $\omega\to 0$ at finite q, and only then take $\mathbf{q}\to 0$, as reported in Fig. 1. Here the term $\{\chi_{\mathbf{jj}}(\mathbf{q}\to 0,\omega=0)-\chi_{\mathbf{jj}}(\mathbf{q},\omega=0)\}$ represents the term $\Delta\chi_T(\mathbf{r},\mathbf{r}',0)$ of Eq. (33) in its Fourier representation. In the absence of magnetic fields the vector potential is regular in $q=0$ for any ω, hence the term $\Delta\chi_T(q,0)$, which is proportional to q^2, does not contribute to the induced current-density for vanishing q. A relation similar to Eq. (33) holds for crystalline systems,

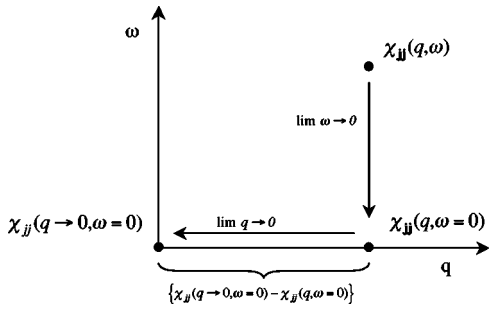

FIG. 1. The order of the limits needed to relate diamagnetic and paramagnetic contributions to the current-current response function.

$$\chi_{\mathbf{jjq}}(\mathbf{r},\mathbf{r}',0) = -\rho_0\delta(\mathbf{r}-\mathbf{r}') + \Delta\chi_{\mathbf{q}}(\mathbf{r},\mathbf{r}',0), \tag{34}$$

where again $\Delta\chi_{\mathbf{q}}(\mathbf{r},\mathbf{r}',0)$ is transverse and of the order of q^2.[17,42] Therefore, we can introduce the following relation for the diamagnetic current-density,

$$\delta\mathbf{j}_{d\mathbf{q}}(\mathbf{r},\omega) = -\delta\mathbf{j}^0_{p\mathbf{q}}(\mathbf{r},\omega) + \Delta\mathbf{j}_{d\mathbf{q}}(\mathbf{r},\omega), \tag{35}$$

where $\delta\mathbf{j}^0_{p\mathbf{q}}(\mathbf{r},\omega)$ is the paramagnetic current-density obtained from the static response, at finite q, to the dynamic perturbation,

$$\begin{aligned}\delta\mathbf{j}^0_{p\mathbf{q}}(\mathbf{r},\omega) = \frac{1}{N_k}\sum_{\mathbf{k},\mathbf{k}'}\sum_{i,a} w_{i\mathbf{k}a\mathbf{k}',+}(0)\\ \times(\delta_{\mathbf{k}',\mathbf{k}+\mathbf{q}}(\psi^*_{i\mathbf{k}}\hat{\mathbf{j}}_{\mathbf{q}}\psi_{a\mathbf{k}'})\langle\psi_{a\mathbf{k}'}|\delta\hat{h}_o(\mathbf{q},\omega)|\psi_{i\mathbf{k}}\rangle\\ + \delta_{\mathbf{k}',\mathbf{k}-\mathbf{q}}(\psi^*_{a\mathbf{k}'}\hat{\mathbf{j}}_{\mathbf{q}}\psi_{i\mathbf{k}})\langle\psi_{i\mathbf{k}}|\delta\hat{h}_o(\mathbf{q},\omega)|\psi_{a\mathbf{k}'}\rangle),\end{aligned} \tag{36}$$

and $\Delta\mathbf{j}_{d\mathbf{q}}(\mathbf{r},\omega)$ is by construction equal to $\delta\mathbf{j}_{d\mathbf{q}}(\mathbf{r},\omega) + \delta\mathbf{j}^0_{p\mathbf{q}}(\mathbf{r},\omega)$, and gives rise to contributions analogous to the Landau diamagnetism. Since we do not treat magnetic fields in this derivation, only the first term on the right-hand side of Eq. (35) is considered and $\Delta\mathbf{j}_{d\mathbf{q}}(\mathbf{r},\omega)$ is neglected in the sequel. Combining Eq. (36) with Eq. (28) for the paramagnetic current-density, the induced physical current is then obtained from

$$\begin{aligned}\delta\mathbf{j}_{\mathbf{q}}(\mathbf{r},\omega) = \frac{1}{N_k}\sum_{\mathbf{k},\mathbf{k}'}\sum_{i,a} w_{i\mathbf{k}a\mathbf{k}',-}(\omega)(\delta_{\mathbf{k}',\mathbf{k}+\mathbf{q}}(\psi^*_{i\mathbf{k}}\hat{\mathbf{j}}_{\mathbf{q}}\psi_{a\mathbf{k}'})\langle\psi_{a\mathbf{k}'}|\delta\hat{h}_e(\mathbf{q},\omega)|\psi_{i\mathbf{k}}\rangle - \delta_{\mathbf{k}',\mathbf{k}-\mathbf{q}}(\psi^*_{a\mathbf{k}'}\hat{\mathbf{j}}_{\mathbf{q}}\psi_{i\mathbf{k}})\langle\psi_{i\mathbf{k}}|\delta\hat{h}_e(\mathbf{q},\omega)|\psi_{a\mathbf{k}'}\rangle)\\ + \frac{1}{N_k}\sum_{\mathbf{k},\mathbf{k}'}\sum_{i,a}[w_{i\mathbf{k}a\mathbf{k}',+}(\omega) - w_{i\mathbf{k}a\mathbf{k}',+}(0)](\delta_{\mathbf{k}',\mathbf{k}+\mathbf{q}}(\psi^*_{i\mathbf{k}}\hat{\mathbf{j}}_{\mathbf{q}}\psi_{a\mathbf{k}'})\langle\psi_{a\mathbf{k}'}|\delta\hat{h}_o(\mathbf{q},\omega)|\psi_{i\mathbf{k}}\rangle\\ + \delta_{\mathbf{k}',\mathbf{k}-\mathbf{q}}(\psi^*_{a\mathbf{k}'}\hat{\mathbf{j}}_{\mathbf{q}}\psi_{i\mathbf{k}})\langle\psi_{i\mathbf{k}}|\delta\hat{h}_o(\mathbf{q},\omega)|\psi_{a\mathbf{k}'}\rangle).\end{aligned} \tag{37}$$

C. Response functions

1. Interband contribution

We will first consider the interband contributions to the induced density and current-density which are obtained from the terms with $a \neq i$ in Eqs. (18) and (37). They can then be written in the following concise form,

$$\begin{pmatrix} \delta\rho_{\mathbf{q}}^{inter} \\ i\delta\mathbf{j}_{\mathbf{q}}^{inter}/\omega \end{pmatrix} = \begin{pmatrix} \chi_{\rho\rho\mathbf{q}}^{inter} & -i\chi_{\rho\mathbf{jq}}^{inter}/\omega \\ i\chi_{\mathbf{j}\rho\mathbf{q}}^{inter}/\omega & (\chi_{\mathbf{jjq}}^{inter} - \chi_{\mathbf{jjq}}^{inter,0})/\omega^2 \end{pmatrix} \cdot \begin{pmatrix} \delta v_{\mathbf{q},eff} \\ i\omega\delta\mathbf{a}_{\mathbf{q},eff}/c \end{pmatrix}, \tag{38}$$

by inserting the equations for the "even" and for the "odd" perturbation, Eqs. (19) and (20). Here the matrix-vector product also includes an integration over a real space coordinate, where the various response kernels take simple forms by using the relations (22) and (23) for $w_{i\mathbf{k}a\mathbf{k}',+}(\omega)$ and $w_{i\mathbf{k}a\mathbf{k}',-}(\omega)$. For the interband contribution to the density-density response function, $\chi_{\rho\rho\mathbf{q}}^{inter}$, we find

$$\begin{aligned}\chi_{\rho\rho\mathbf{q}}^{inter}(\mathbf{r},\mathbf{r}',\omega) = \frac{1}{N_k}\sum_{\mathbf{k},\mathbf{k}'}\sum_{ia} w_{i\mathbf{k}a\mathbf{k}',+}(\omega)\{&\delta_{\mathbf{k}'\mathbf{k}+\mathbf{q}}[\psi_{i\mathbf{k}}^*(\mathbf{r})\hat{\rho}_{\mathbf{q}}\psi_{a\mathbf{k}'}(\mathbf{r})] \\ &\times[\psi_{a\mathbf{k}'}^*(\mathbf{r}')\hat{\rho}'_{-\mathbf{q}}\psi_{i\mathbf{k}}(\mathbf{r}')] \\ &+ \delta_{\mathbf{k}'\mathbf{k}-\mathbf{q}}[\psi_{a\mathbf{k}'}^*(\mathbf{r})\hat{\rho}_{\mathbf{q}}\psi_{i\mathbf{k}}(\mathbf{r})] \\ &\times[\psi_{i\mathbf{k}}^*(\mathbf{r}')\hat{\rho}'_{-\mathbf{q}}\psi_{a\mathbf{k}'}(\mathbf{r}')]\}.\end{aligned} \tag{39}$$

For the contributions to the density-current and current-density response functions, $\chi_{\rho\mathbf{jq}}^{inter}$ and $\chi_{\mathbf{j}\rho\mathbf{q}}^{inter}$, the equations become

$$\begin{aligned}-\frac{i}{\omega}\chi_{\rho\mathbf{jq}}^{inter}(\mathbf{r},\mathbf{r}',\omega) = \frac{1}{N_k}\sum_{\mathbf{k},\mathbf{k}'}\sum_{ia} w_{i\mathbf{k}a\mathbf{k}',+}(\omega) &\times\Bigg(\delta_{\mathbf{k}'\mathbf{k}+\mathbf{q}}[\psi_{i\mathbf{k}}^*(\mathbf{r})\hat{\rho}_{\mathbf{q}}\psi_{a\mathbf{k}'}(\mathbf{r})] \\ &\times\frac{i\psi_{a\mathbf{k}'}^*(\mathbf{r}')\hat{\mathbf{j}}'_{-\mathbf{q}}\psi_{i\mathbf{k}}(\mathbf{r}')}{\epsilon_{i\mathbf{k}}-\epsilon_{a\mathbf{k}'}} \\ &+ \delta_{\mathbf{k}'\mathbf{k}-\mathbf{q}}[\psi_{a\mathbf{k}'}^*(\mathbf{r})\hat{\rho}_{\mathbf{q}}\psi_{i\mathbf{k}}(\mathbf{r})] \\ &\times\frac{i\psi_{i\mathbf{k}}^*(\mathbf{r}')\hat{\mathbf{j}}'_{-\mathbf{q}}\psi_{a\mathbf{k}'}(\mathbf{r}')}{\epsilon_{a\mathbf{k}'}-\epsilon_{i\mathbf{k}}}\Bigg),\end{aligned} \tag{40}$$

$$\begin{aligned}\frac{i}{\omega}\chi_{\mathbf{j}\rho\mathbf{q}}^{inter}(\mathbf{r},\mathbf{r}',\omega) = \frac{1}{N_k}\sum_{\mathbf{k},\mathbf{k}'}\sum_{ia} w_{i\mathbf{k}a\mathbf{k}',+}(\omega) &\times\Bigg(\delta_{\mathbf{k}'\mathbf{k}+\mathbf{q}}\frac{i\psi_{i\mathbf{k}}^*(\mathbf{r})\hat{\mathbf{j}}_{\mathbf{q}}\psi_{a\mathbf{k}'}(\mathbf{r})}{\epsilon_{a\mathbf{k}'}-\epsilon_{i\mathbf{k}}} \\ &\times[\psi_{a\mathbf{k}'}^*(\mathbf{r}')\hat{\rho}'_{-\mathbf{q}}\psi_{i\mathbf{k}}(\mathbf{r}')] + \delta_{\mathbf{k}'\mathbf{k}-\mathbf{q}} \\ &\times\frac{i\psi_{a\mathbf{k}'}^*(\mathbf{r})\hat{\mathbf{j}}_{\mathbf{q}}\psi_{i\mathbf{k}}(\mathbf{r})}{\epsilon_{i\mathbf{k}}-\epsilon_{a\mathbf{k}'}}[\psi_{i\mathbf{k}}^*(\mathbf{r}')\hat{\rho}'_{-\mathbf{q}}\psi_{a\mathbf{k}'}(\mathbf{r}')]\Bigg),\end{aligned} \tag{41}$$

and finally for the interband contribution to the combination of the current-current response function and its static value, respectively $\chi_{\mathbf{jjq}}^{inter}$ and $\chi_{\mathbf{jjq}}^{inter,0}$, the result is

$$\begin{aligned}\frac{1}{\omega^2}[\chi_{\mathbf{jjq}}^{inter}(\mathbf{r},\mathbf{r}',\omega) - \chi_{\mathbf{jjq}}^{inter}(\mathbf{r},\mathbf{r}',\omega=0)] = \frac{1}{N_k}\sum_{\mathbf{k},\mathbf{k}'}\sum_{ia} w_{i\mathbf{k}a\mathbf{k}',+}(\omega) \\ \times\Bigg(\delta_{\mathbf{k}'\mathbf{k}+\mathbf{q}}\frac{i\psi_{i\mathbf{k}}^*(\mathbf{r})\hat{\mathbf{j}}_{\mathbf{q}}\psi_{a\mathbf{k}'}(\mathbf{r})}{\epsilon_{a\mathbf{k}'}-\epsilon_{i\mathbf{k}}} \otimes \frac{i\psi_{a\mathbf{k}'}^*(\mathbf{r}')\hat{\mathbf{j}}'_{-\mathbf{q}}\psi_{i\mathbf{k}}(\mathbf{r}')}{\epsilon_{i\mathbf{k}}-\epsilon_{a\mathbf{k}'}} \\ + \delta_{\mathbf{k}'\mathbf{k}-\mathbf{q}}\frac{i\psi_{a\mathbf{k}'}^*(\mathbf{r})\hat{\mathbf{j}}_{\mathbf{q}}\psi_{i\mathbf{k}}(\mathbf{r})}{\epsilon_{i\mathbf{k}}-\epsilon_{a\mathbf{k}'}} \otimes \frac{i\psi_{i\mathbf{k}}^*(\mathbf{r}')\hat{\mathbf{j}}'_{-\mathbf{q}}\psi_{a\mathbf{k}'}(\mathbf{r}')}{\epsilon_{a\mathbf{k}'}-\epsilon_{i\mathbf{k}}}\Bigg).\end{aligned} \tag{42}$$

The ω dependence in the above expressions for the various interband contributions is governed by the common factor $w_{i\mathbf{k}a\mathbf{k}',+}(\omega)$, which is a well-behaved function of ω and q for ω smaller than the (indirect) energy gap between the different occupied and unoccupied bands. The various interband contributions to the response functions have then the following ω dependence:

$$\chi_{\rho\rho\mathbf{q}}^{inter} \propto 1,$$

$$\chi_{\rho\mathbf{jq}}^{inter}, \chi_{\mathbf{j}\rho\mathbf{q}}^{inter} \propto \omega,$$

$$(\chi_{\mathbf{jjq}}^{inter} - \chi_{\mathbf{jjq}}^{0,inter}) \propto \omega^2.$$

In the limit of vanishing q the set of equations (39)–(42) reduces to the one used in the case of nonmetallic crystalline systems[12,13] for which we need to consider only fully occupied bands i and fully unoccupied bands a. However, in metallic crystals, we have to consider also the contribution from partially occupied and/or unoccupied bands, for which $\mathbf{k}$-space integrations are restricted to just a part of the Brillouin zone cut off by the Fermi surface.

2. Intraband contribution

Let us consider now the intraband contributions to Eqs. (18) and (37) that are given by the terms with $a=i$ in the summation over the energy bands. By changing variables from $\{\mathbf{k}',\mathbf{k}\}=\{\mathbf{k}-\mathbf{q},\mathbf{k}\}$ to $\{\mathbf{k},\mathbf{k}+\mathbf{q}\}$ in the second and fourth terms in Eq. (18) we obtain

$$\begin{aligned}\delta\rho_{\mathbf{q}}^{intra}(\mathbf{r},\omega) = \frac{1}{N_k}\sum_{i,\mathbf{k}} 2w_{i\mathbf{k}i\mathbf{k}+\mathbf{q},+}(\omega)[\psi_{i\mathbf{k}}^*(\mathbf{r})\hat{\rho}_{\mathbf{q}}\psi_{i\mathbf{k}+\mathbf{q}}(\mathbf{r})] \\ \times\langle\psi_{i\mathbf{k}+\mathbf{q}}|\delta\hat{h}_e(\mathbf{q},\omega)|\psi_{i\mathbf{k}}\rangle + \frac{1}{N_k}\sum_{i,\mathbf{k}} 2w_{i\mathbf{k}i\mathbf{k}+\mathbf{q},-}(\omega) \\ \times[\psi_{i\mathbf{k}}^*(\mathbf{r})\hat{\rho}_{\mathbf{q}}\psi_{a\mathbf{k}+\mathbf{q}}(\mathbf{r})]\langle\psi_{i\mathbf{k}+\mathbf{q}}|\delta\hat{h}_o(\mathbf{q},\omega)|\psi_{i\mathbf{k}}\rangle,\end{aligned} \tag{43}$$

where we have used that $w_{i\mathbf{k}i\mathbf{k}+\mathbf{q},\pm}(\omega) = \pm w_{i\mathbf{k}+\mathbf{q}i\mathbf{k},\pm}(\omega)$. Operating in a similar way in Eq. (37) for the induced current-density we arrive at

$$\delta\mathbf{j}_{\mathbf{q}}^{intra}(\mathbf{r},\omega)=\frac{1}{N_k}\sum_{i,\mathbf{k}}2w_{i\mathbf{k}i\mathbf{k}+\mathbf{q},-}(\omega)[\psi_{i\mathbf{k}}^{*}(\mathbf{r})\hat{\mathbf{j}}_{\mathbf{q}}\psi_{i\mathbf{k}+\mathbf{q}}(\mathbf{r})]\times\langle\psi_{i\mathbf{k}+\mathbf{q}}|\delta\hat{h}_e(\mathbf{q},\omega)|\psi_{i\mathbf{k}}\rangle+\frac{1}{N_k}\sum_{i,\mathbf{k}}2[w_{i\mathbf{k}a\mathbf{k}+\mathbf{q},+}(\omega)-w_{i\mathbf{k}i\mathbf{k}+\mathbf{q},+}(0)]\times[\psi_{i\mathbf{k}}^{*}(\mathbf{r})\hat{\mathbf{j}}_{\mathbf{q}}\psi_{i\mathbf{k}+\mathbf{q}}(\mathbf{r})]\langle\psi_{i\mathbf{k}+\mathbf{q}}|\delta\hat{h}_o(\mathbf{q},\omega)|\psi_{i\mathbf{k}}\rangle. \tag{44}$$

These expressions can be written in the following concise form,

$$i\omega\begin{pmatrix}\omega/q\,\delta\rho_{\mathbf{q}}^{intra}\\ \delta\mathbf{j}_{\mathbf{q}}^{intra}\end{pmatrix}=\begin{pmatrix}\omega^2/q^2\chi_{\rho\rho\mathbf{q}}^{intra} & \omega/q\chi_{\rho\mathbf{j}\mathbf{q}}^{intra}\\ \omega/q\chi_{\mathbf{j}\rho\mathbf{q}}^{intra} & \chi_{\mathbf{j}\mathbf{j}\mathbf{q}}^{intra}-\chi_{\mathbf{j}\mathbf{j}\mathbf{q}}^{intra,0}\end{pmatrix}\cdot\begin{pmatrix}iq\delta v_{\mathbf{q},eff}\\ i\omega\delta\mathbf{a}_{\mathbf{q},eff}/c\end{pmatrix}, \tag{45}$$

where the various response kernels are given in the following set of equations. For the intraband contribution to the density-density response kernel, $\chi_{\rho\rho\mathbf{q}}^{intra}$, we get,

$$\frac{\omega^2}{q^2}\chi_{\rho\rho\mathbf{q}}^{intra}(\mathbf{r},\mathbf{r}',\omega)=\frac{2}{N_k}\sum_{i\mathbf{k}}\frac{\omega^2}{q^2}w_{i\mathbf{k}i\mathbf{k}+\mathbf{q},+}(\omega)[\psi_{i\mathbf{k}}^{*}(\mathbf{r})\hat{\rho}_{\mathbf{q}}\psi_{i\mathbf{k}+\mathbf{q}}(\mathbf{r})]\times[\psi_{i\mathbf{k}+\mathbf{q}}^{*}(\mathbf{r}')\hat{\rho}'_{-\mathbf{q}}\psi_{i\mathbf{k}}(\mathbf{r}')]. \tag{46}$$

Similarly for the contributions to the density-current and current-density kernels, $\chi_{\rho\mathbf{j}\mathbf{q}}^{intra}$ and $\chi_{\mathbf{j}\rho\mathbf{q}}^{intra}$, the expressions are

$$\frac{\omega}{q}\chi_{\rho\mathbf{j}q}^{intra}(\mathbf{r},\mathbf{r}',\omega)=\frac{2}{N_k}\sum_{i\mathbf{k}}\frac{\omega^2}{q}\frac{w_{i\mathbf{k}i\mathbf{k}+\mathbf{q},+}(\omega)}{\epsilon_{i\mathbf{k}+\mathbf{q}}-\epsilon_{i\mathbf{k}}}[\psi_{i\mathbf{k}}^{*}(\mathbf{r})\hat{\rho}_{\mathbf{q}}\psi_{i\mathbf{k}+\mathbf{q}}(\mathbf{r})]\times[\psi_{i\mathbf{k}+\mathbf{q}}^{*}(\mathbf{r}')\hat{\mathbf{j}}'_{-\mathbf{q}}\psi_{i\mathbf{k}}(\mathbf{r}')], \tag{47}$$

$$\frac{\omega}{q}\chi_{\mathbf{j}\rho\mathbf{q}}^{intra}(\mathbf{r},\mathbf{r}',\omega)=\frac{2}{N_k}\sum_{i\mathbf{k}}\frac{\omega^2}{q}\frac{w_{i\mathbf{k}i\mathbf{k}+\mathbf{q},+}(\omega)}{\epsilon_{i\mathbf{k}+\mathbf{q}}-\epsilon_{i\mathbf{k}}}[\psi_{i\mathbf{k}}^{*}(\mathbf{r})\hat{\mathbf{j}}_{\mathbf{q}}\psi_{i\mathbf{k}+\mathbf{q}}(\mathbf{r})]\times[\psi_{i\mathbf{k}+\mathbf{q}}^{*}(\mathbf{r}')\hat{\rho}'_{-\mathbf{q}}\psi_{i\mathbf{k}}(\mathbf{r}')]. \tag{48}$$

Finally, for the intraband contribution to the combination of the current-current response function and its static value, respectively $\chi_{\mathbf{j}\mathbf{j}\mathbf{q}}^{intra}$ and $\chi_{\mathbf{j}\mathbf{j}\mathbf{q}}^{intra,0}$, we have

$$\chi_{\mathbf{j}\mathbf{j}\mathbf{q}}^{intra}(\mathbf{r},\mathbf{r}',\omega)-\chi_{\mathbf{j}\mathbf{j}\mathbf{q}}^{intra}(\mathbf{r},\mathbf{r}',\omega=0)=\frac{2}{N_k}\sum_{i\mathbf{k}}\omega^2\frac{w_{i\mathbf{k}i\mathbf{k}+\mathbf{q},+}(\omega)}{(\epsilon_{i\mathbf{k}+\mathbf{q}}-\epsilon_{i\mathbf{k}})^2}\times[\psi_{i\mathbf{k}}^{*}(\mathbf{r})\hat{\mathbf{j}}_{\mathbf{q}}\psi_{i\mathbf{k}+\mathbf{q}}(\mathbf{r})]\otimes[\psi_{i\mathbf{k}+\mathbf{q}}^{*}(\mathbf{r}')\hat{\mathbf{j}}'_{-\mathbf{q}}\psi_{i\mathbf{k}}(\mathbf{r}')]. \tag{49}$$

In this paper we will only consider the optical limit, i.e., the limit of vanishing q (but finite ω), for which we can evaluate the weights $w_{i\mathbf{k}i\mathbf{k}+\mathbf{q},+}(\omega)$ using the two relations

$$\epsilon_{i\mathbf{k}}-\epsilon_{i\mathbf{k}+\mathbf{q}}\simeq-q(\nabla_{\mathbf{k}}\epsilon_{i\mathbf{k}}\cdot\hat{\mathbf{q}}), \tag{50}$$

$$f_{i\mathbf{k}}-f_{i\mathbf{k}+\mathbf{q}}=f(\epsilon_{i\mathbf{k}})-f(\epsilon_{i\mathbf{k}+\mathbf{q}})\simeq-q\frac{df}{d\epsilon}(\nabla_{\mathbf{k}}\epsilon_{i\mathbf{k}}\cdot\hat{\mathbf{q}}). \tag{51}$$

We can then write for the common factor $2\omega^2/q^2w_{i\mathbf{k}i\mathbf{k}+\mathbf{q},+}(\omega)$,

$$2\frac{\omega^2}{q^2}w_{i\mathbf{k}i\mathbf{k}+\mathbf{q},+}(\omega)\simeq\frac{df}{d\epsilon}\frac{\omega^2(\nabla_{\mathbf{k}}\epsilon_{i\mathbf{k}}\cdot\hat{\mathbf{q}})^2}{q^2(\nabla_{\mathbf{k}}\epsilon_{i\mathbf{k}}\cdot\hat{\mathbf{q}})^2-(\omega+i\eta)^2}. \tag{52}$$

The nonanalytic behavior of the intraband response functions at the origin of the q-ω plane is now made explicit. In the limit of q to zero at finite ω this factor becomes independent of ω and equal to $df/d\epsilon(\nabla_{\mathbf{k}}\epsilon_{i\mathbf{k}}\cdot\hat{\mathbf{q}})^2$, whereas in the reverse order of limits the factor is zero. It immediately becomes clear that the intraband response functions show the following ω and q dependence at small q but finite ω,

$$\chi_{\rho\rho\mathbf{q}}^{intra}\propto q^2/\omega^2,$$

$$\chi_{\rho\mathbf{j}\mathbf{q}}^{intra},\chi_{\mathbf{j}\rho\mathbf{q}}^{intra}\propto q/\omega,$$

$$\chi_{\mathbf{j}\mathbf{j}\mathbf{q}}^{intra}-\chi_{\mathbf{j}\mathbf{j}\mathbf{q}}^{0,intra}\propto 1.$$

D. The SCF equations

In the previous section we derived expressions for the induced density and current-density as result of a given set of vector and scalar potentials. To complete the self-consistent-field scheme of Kohn and Sham[3] we have to express the induced potentials in terms of the induced density and current-density. In order to do this it is important to separate microscopic and macroscopic components of these densities and to show how they lead to the microscopic and macroscopic contributions to the induced potentials. We will do this first for the Hartree term and then for the exchange-correlation contributions. We start by identifying the microscopic and macroscopic components of the density. Since both the inter- and intraband contributions to $\delta\rho_{\mathbf{q}}(\mathbf{r},\omega)$ are lattice periodic, we can write the total induced density as a Fourier series expansion,

$$\delta\rho(\mathbf{r},\omega)=e^{i\mathbf{q}\cdot\mathbf{r}}\delta\rho_{\mathbf{q}}(\mathbf{r},\omega)=e^{i\mathbf{q}\cdot\mathbf{r}}\sum_{\mathbf{G}}\delta\rho_{\mathbf{q}+\mathbf{G}}(\omega)e^{i\mathbf{G}\cdot\mathbf{r}}. \tag{53}$$

Here the term with $\mathbf{G}=0$ is equal to the macroscopic density defined in Eq. (17). The remaining terms with $\mathbf{G}\neq\mathbf{0}$ together constitute the macroscopic density. One usually assumes[18,19] that a similar expansion exists for the Hartree potential which can then be written as

$$\delta v_H(\mathbf{r},\omega)=4\pi e^{i\mathbf{q}\cdot\mathbf{r}}\left(\frac{\delta\rho_{\mathbf{q}+\mathbf{0}}(\omega)}{q^2}+\sum_{\mathbf{G}\neq\mathbf{0}}\frac{\delta\rho_{\mathbf{q}+\mathbf{G}}(\omega)}{|\mathbf{q}+\mathbf{G}|^2}e^{i\mathbf{G}\cdot\mathbf{r}}\right). \tag{54}$$

One can then define the microscopic scalar potential $\delta v_{H,mic}$ as

$$\delta v_{H,mic}(\mathbf{r},\omega)=4\pi e^{i\mathbf{q}\cdot\mathbf{r}}\sum_{\mathbf{G}\neq\mathbf{0}}\frac{\delta\rho_{\mathbf{q}+\mathbf{G}}(\omega)}{|\mathbf{q}+\mathbf{G}|^2}e^{i\mathbf{G}\cdot\mathbf{r}}, \tag{55}$$

whereas the term $e^{i\mathbf{q}\cdot\mathbf{r}}\delta v_{\mathbf{q}+\mathbf{0}}\doteq 4\pi e^{i\mathbf{q}\cdot\mathbf{r}}\delta\rho_{\mathbf{q}+\mathbf{0}}/q^2$ represents a macroscopic field. In the TDCDFT approach this term will be gauge-transformed to a macroscopic vector potential,

$$\frac{i\omega}{c}\delta\mathbf{a}_{H,mac}(\mathbf{r},\omega) = \nabla\,(e^{i\mathbf{q}\cdot\mathbf{r}}\delta v_{\mathbf{q}+\mathbf{0}}(\omega)) = 4\pi i\hat{\mathbf{q}}\left(\frac{\delta\rho_{\mathbf{q}+\mathbf{0}}(\omega)}{q}\right)e^{i\mathbf{q}\cdot\mathbf{r}}. \tag{56}$$

As Kootstra *et al.* have shown, this field is sample-shape dependent. In their approach this contribution is, by construction, already contained in the total macroscopic vector potential, which describes the macroscopic electric field, and which is kept fixed [Eqs. (8) and (9)].[12] Note that we do not evaluate the microscopic scalar potential using the Fourier series expansion, as this series converges extremely slowly for real densities. Instead we make use of the screening technique described by Kootstra *et al.*[12] In the effective one-electron scheme of Kohn and Sham the effective potentials $\{\delta v_{eff}, \delta\mathbf{a}_{eff}\}$ also contain exchange-correlation contributions. For the total exchange-correlation scalar potential we write

$$\delta v_{xc}(\mathbf{r},\omega) = \int f_{xc}(\mathbf{r},\mathbf{r}',\omega)\,\delta\rho(\mathbf{r}',\omega)d\mathbf{r}', \tag{57}$$

in which we will use the adiabatic local density approximation (ALDA) for the exchange-correlation kernel $f_{xc}(\mathbf{r},\mathbf{r}',\omega)$,

$$f_{xc}(\mathbf{r},\mathbf{r}',\omega) = f_{xc}^{ALDA}(\mathbf{r},\mathbf{r}') = \delta(\mathbf{r}-\mathbf{r}')\ \left.\frac{dv_{xc}^{LDA}(\rho)}{d\rho}\right|_{\rho=\rho_0(\mathbf{r})}. \tag{58}$$

In our scheme all other exchange-correlation effects are to be included in the exchange-correlation vector potential. As the induced density is a functional of the induced current-density through the continuity equation, we can formally write this vector potential as a pure functional of the induce current-density,

$$\delta\mathbf{a}_{xc}(\mathbf{r},\omega) = \int \mathbf{f}_{xc}(\mathbf{r},\mathbf{r}',\omega)\cdot\delta\mathbf{j}(\mathbf{r}',\omega)\ d\mathbf{r}'. \tag{59}$$

As in Ref. 12, we split also these contributions into microscopic and macroscopic components. To achieve this we choose to retain only terms linear in the microscopic induced density in the microscopic exchange-correlation scalar potential, and to gauge-transform all terms linear in the macroscopic induced density and those linear in the induced current-density to the exchange-correlation vector potential. This is possible because we consider only the linear response. In this way we keep contact with the ordinary TDDFT formulation. This vector potential will contain in general both microscopic and macroscopic components. In the gauge described above the effective potentials take the following form,

$$\delta v_{eff,mic} = \delta v_{H,mic} + \delta v_{xc}^{ALDA}[\delta\rho_{mic}], \tag{60}$$

$$\delta\mathbf{a}_{\text{eff}} = \delta\mathbf{a}_{mac} + \delta\mathbf{a}_{xc}[\delta\mathbf{j}] - \frac{ic}{\omega}\nabla\,\delta v_{xc}^{ALDA}[\delta\rho_{mac}]. \tag{61}$$

Using Eq. (57) the last term in Eq. (61) can be written as,

$$-\frac{ic}{\omega}\nabla\,\delta v_{xc}^{ALDA}[\delta\rho_{mac}](\mathbf{r},\omega) = -\frac{ic}{\omega}\left[(i\mathbf{q}+\nabla)\frac{dv_{xc}^{LDA}}{d\rho}(\rho_0(\mathbf{r}))\right] \times\delta\rho_{\mathbf{q}+\mathbf{0}}(\omega)e^{i\mathbf{q}\cdot\mathbf{r}}. \tag{62}$$

In the ALDA approximation used in this paper we will neglect the exchange-correlation contribution $\delta\mathbf{a}_{xc}[\delta\mathbf{j}]$ in the effective vector potential, and retain only the macroscopic part of the other terms. Then Eq. (61) becomes,

$$\delta\mathbf{a}_{eff,mac}(\mathbf{r},\omega) = \delta\mathbf{a}_{mac}(\mathbf{r},\omega) + c\hat{\mathbf{q}}\frac{q}{\omega}\left(\frac{1}{V}\int_V\frac{dv_{xc}^{LDA}}{d\rho}(\rho_0(\mathbf{r}))d\mathbf{r}\right)\delta\rho_{\mathbf{q}+\mathbf{0}}e^{i\mathbf{q}\cdot\mathbf{r}}, \tag{63}$$

where in calculating the cell average the contribution of the gradient in Eq. (62) vanishes due to the lattice-periodicity of the ground-state density $\rho_0(\mathbf{r})$.

The separation of the induced potentials in microscopic and macroscopic terms as discussed above is based on the separation of the induced density into microscopic and macroscopic components. We will now describe how inter- and intraband processes contribute to the microscopic and macroscopic parts of the induced density. To achieve this we refer to Eq. (15) and analyze first the factor $\psi_{i\mathbf{k}}^*(\mathbf{r})\hat{\rho}_{\mathbf{q}}\psi_{a\mathbf{k}+\mathbf{q}}(\mathbf{r})$. Using the expression for the Bloch functions and the definition of the $\hat{\rho}_{\mathbf{q}}$ operator, it becomes evident that this factor is lattice periodic and can be written as a Fourier series expansion,

$$\psi_{i\mathbf{k}}^*(\mathbf{r})\hat{\rho}_{\mathbf{q}}\psi_{a\mathbf{k}+\mathbf{q}}(\mathbf{r}) = u_{i\mathbf{k}}^*(\mathbf{r})e^{-i\mathbf{k}\cdot\mathbf{r}}e^{-i\mathbf{q}\cdot\mathbf{r}}u_{a\mathbf{k}+\mathbf{q}}(\mathbf{r})e^{i(\mathbf{k}+\mathbf{q})\cdot\mathbf{r}} = \frac{1}{V}\sum_{\mathbf{G}}C_{ia\mathbf{G}}(\mathbf{q})e^{i\mathbf{G}\cdot\mathbf{r}}. \tag{64}$$

We can now use the following relation obtained using the $\mathbf{k}\cdot\mathbf{p}$ method,[43]

$$u_{a\mathbf{k}+\mathbf{q}}(\mathbf{r}) = (1+i\boldsymbol{\alpha}_{a\mathbf{k}}\cdot\mathbf{q})u_{a\mathbf{k}}(\mathbf{r}) + \sum_{n\neq a}\frac{\langle\psi_{n\mathbf{k}}|\hat{\mathbf{p}}|\psi_{a\mathbf{k}}\rangle\cdot\mathbf{q}}{\epsilon_{a\mathbf{k}}-\epsilon_{n\mathbf{k}}}\cdot u_{n\mathbf{k}}(\mathbf{r}) + \mathcal{O}(q^2), \tag{65}$$

where, in the nondegenerate case, $\boldsymbol{\alpha}_{a\mathbf{k}}$ can be chosen to be a continuous and periodic function of $\mathbf{k}$. For the coefficient $C_{ia\mathbf{G}=\mathbf{0}}(\mathbf{q})$, which determines the value of the macroscopic density $\delta\rho_{\mathbf{q}+\mathbf{0}}(\omega)$, in Eq. (53) we then get

$$C_{ia\mathbf{G}=\mathbf{0}}(\mathbf{q}) = \int u_{i\mathbf{k}}^*(\mathbf{r})u_{a\mathbf{k}+\mathbf{q}}(\mathbf{r})\ d\mathbf{r} = (1+i\alpha_{a\mathbf{k}}\cdot\mathbf{q})\delta_{ia} + \frac{\langle\psi_{i\mathbf{k}}|\hat{\mathbf{p}}|\psi_{a\mathbf{k}}\rangle\cdot\mathbf{q}}{\epsilon_{a\mathbf{k}}-\epsilon_{i\mathbf{k}}}\cdot(1-\delta_{ia}) + \mathcal{O}(q^2), \tag{66}$$

where we made use of the orthogonality of the Bloch functions. The coefficients $C_{ia\mathbf{G}\neq\mathbf{0}}(\mathbf{q})$ that determine the microscopic density are in general of order 1. We consider first the q dependence of the interband contribution to the macroscopic induced density, by inspecting Eq. (38) for $\delta\rho_{\mathbf{q}}^{inter}$ and Eqs. (39) and (40) for the interband contribution to the response functions. In these last two expressions the weights

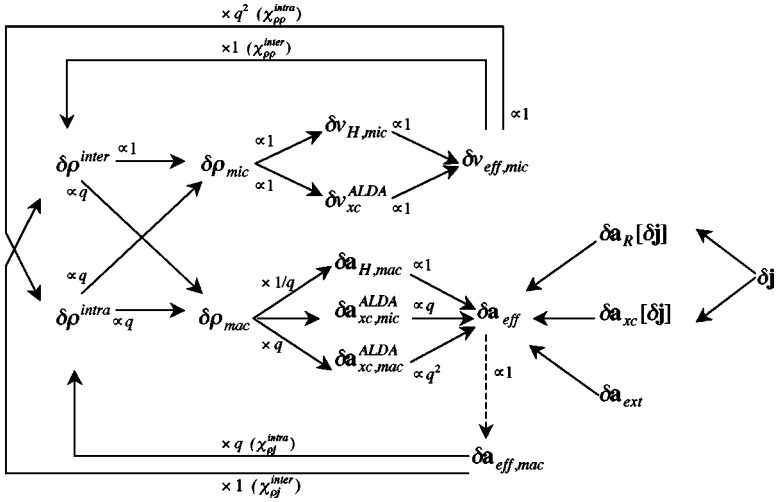

FIG. 2. Schematic representation of the self-consistent field (SCF) calculation of microscopic and macroscopic parts of the induced density. The leading order in powers of q is indicated near the variables by the "$\propto$" sign. The arrows indicate the contributions to each variable, where the "$\times$" sign indicates the order in q gained through some multiplicative factor. The inter- and intraband contributions to the induced density both contribute to the microscopic and macroscopic components of this density. In the microscopic Coulomb gauge only the microscopic density gives rise to the microscopic effective scalar potential via the microscopic Hartree term and the ALDA xc-term. The macroscopic density as well as the current-density contribute in various ways to the effective vector potential. The dashed line indicates that the self-consistent loop is not completed as we keep the macroscopic effective vector potential fixed. For more details and discussions see the text.

$w_{i\mathbf{k}a\mathbf{k}+\mathbf{q},+}$ have a leading term of order 1 in the expansion in orders of q, as $i \neq a$. From the expressions (64) and (66) it follows that for $i \neq a$ the uniform component of the factor $\psi^*_{i\mathbf{k}}\hat{\rho}_{\mathbf{q}}\psi_{a\mathbf{k}+\mathbf{q}} = C_{ia\mathbf{G}=\mathbf{0}}(\mathbf{q})$ is of order q. Hence the interband contribution to the macroscopic induced density is one order in q higher than the off-diagonal matrix elements of the perturbations $\hat{\rho}_{-\mathbf{q}}\delta v_{\mathbf{q},eff}$ and $i\omega/c\hat{\mathbf{j}}_{-\mathbf{q}}\cdot\delta\mathbf{a}_{\mathbf{q},eff}$. The microscopic part is, on the other hand, of the same order as these matrix elements. For the intraband case we refer to Eqs. (45)–(47). Here the uniform component of $\psi^*_{i\mathbf{k}}\hat{\rho}_{\mathbf{q}}\psi_{a\mathbf{k}+\mathbf{q}}$ is of order 1, as here $i=a$ in Eq. (66), and also the common factor $\omega^2/q^2 w_{i\mathbf{k}i\mathbf{k}+\mathbf{q},+}(\omega)$, as defined in Eq. (52), is of this order. Together with Eq. (45) we can now conclude that both the microscopic and macroscopic components of the intraband induced density are two orders in q higher than the diagonal matrix elements of the perturbation $\hat{\rho}_{-\mathbf{q}}\delta v_{\mathbf{q},eff}$, and one order in q higher than those of the perturbation $i\omega/c\hat{\mathbf{j}}_{-\mathbf{q}}\cdot\delta\mathbf{a}_{\mathbf{q},eff}$.

The relations derived above constitute a set of self-consistent-field equations for the induced density that are depicted schematically in Fig. 2. The self-consistent loops involving the macroscopic effective vector potential do not need to be completed as we keep this macroscopic potential fixed to calculate the optical response. Assuming that both the effective microscopic scalar potential and the effective macroscopic vector potential are of order 1, we can see that the contribution of the interband processes to the microscopic density is of order 1 and that to the macroscopic density is of order q. In a similar way we can conclude that the contributions of the intraband processes to the microscopic and macroscopic densities are both of order q. From Eqs. (55) and (57) within the ALDA it immediately becomes clear that a microscopic density of order 1 leads to an effective microscopic scalar potential of order 1, consistent with the initial assumption. On the other hand, a macroscopic density of order q will lead according to Eq. (56) to a macroscopic contribution to the effective vector potential of order 1, again consistent with the initial assumption. Within the ALDA the contribution of a macroscopic density of order q will lead to an exchange-correlation vector potential of order q with a uniform component of order q^2 [Eq. (62)]. The latter two contributions hence vanish in the optical limit. Using the scaling introduced in Eq. (45) all the variables acquire the same order in q as depicted in Fig. 3.

Now it also becomes clear that in the optical limit the self-consistent loops for the microscopic and macroscopic induced density become decoupled. Since the contribution to

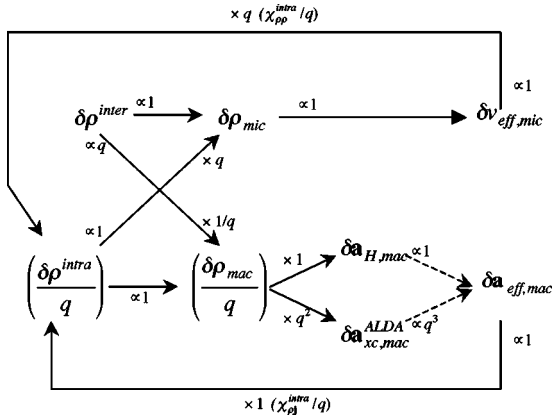

FIG. 3. Schematic representation of the main changes in the calculation of the intraband induced density after the scaling to $\delta\rho^{intra}/q$ and $\delta\rho_{mac}/q$. The symbols used are similar as in Fig. 2. Note that not all the relations are indicated but only those involving the rescaled variables.

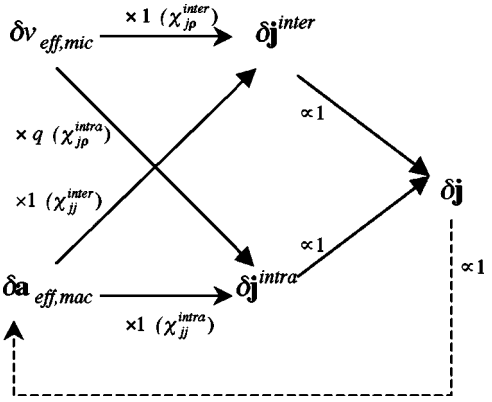

FIG. 4. Schematic representation of post-SCF calculations of inter- and intraband contributions to the induced current-density. Here the dashed line indicates the additional SCF loop that needs to be considered when taking into account a current-dependent exchange-correlation functional.

the scaled intraband induced density $\delta\rho_{\mathbf{q}}^{intra}/q$ that is due to the microscopic effective scalar potential is of order q, it vanishes in the optical limit. Accounting for the scaling, the intraband contribution to the microscopic density is of order q and vanishes for q going to zero. The interband contribution to the scaled macroscopic density $\delta\rho_{\mathbf{q},mac}/q$ is, however, of order 1. Therefore we can conclude that the SCF for the microscopic density can be solved independently from the SCF for the macroscopic density, but that the reverse is not true. It is now clear how we can solve the optical response of metallic systems within the ALDA. First, for a given macroscopic vector potential, we need to solve the equations for the microscopic induced density and microscopic effective scalar potential self-consistently. With both the perturbing potentials now known, we can calculate the macroscopic induced density and the induced current-density.

E. The macroscopic dielectric function

The macroscopic dielectric function $\epsilon(\mathbf{q},\omega)$ is a tensor that can be expressed as

$$\epsilon(\mathbf{q},\omega) = 1 + 4\pi\chi_e(\mathbf{q},\omega), \tag{67}$$

where the the macroscopic susceptibility $\chi_e(\mathbf{q},\omega)$ can be obtained in terms of the total induced macroscopic current via

$$\chi_e(\mathbf{q},\omega)\cdot\hat{\mathbf{e}} = \left(\frac{-i}{\omega V}\int \delta\mathbf{j}_{\mathbf{q}}(\mathbf{r},\omega)\,d\mathbf{r}\right)\Bigg|_{(i\omega/c)\delta\mathbf{a}_{mac,\mathbf{q}}=\hat{\mathbf{e}}}. \tag{68}$$

In Fig. 4 we report schematically the post-SCF calculation for the induced current-density. In the optical limit, i.e., for $q=0$, the expression for the dielectric function takes a simple form. In the limit of $q\to 0$ the microscopic scalar potential does not contribute to the intraband current-density. Thus, in this limit and within the ALDA, the inter- and intraband contributions to the induced current-density can be calculated independently. From Eq. (38) we can obtain the interband contribution to the electric susceptibility by repeating the SCF calculation for the uniform macroscopic field in the three Cartesian directions $\hat{\mathbf{e}}$,

$$\chi_e^{inter}(\mathbf{q}=\mathbf{0},\omega)\cdot\hat{\mathbf{e}} = \left(\frac{-i}{\omega V}\int \delta\mathbf{j}^{inter}_{\mathbf{q}=\mathbf{0}}(\mathbf{r},\omega)\,d\mathbf{r}\right)\Bigg|_{(i\omega/c)\delta\mathbf{a}_{mac,\mathbf{q}=\mathbf{0}}=\hat{\mathbf{e}}}. \tag{69}$$

From Eqs. (45) and (63) the macroscopic part of the intraband contribution to the induced current can be written as

$$\sigma^{intra}(\mathbf{q}=\mathbf{0},\omega)\cdot\hat{\mathbf{e}} = \left(\frac{1}{V}\int \delta\mathbf{j}^{intra}_{\mathbf{q}=\mathbf{0}}(\mathbf{r},\omega)\,d\mathbf{r}\right)\Bigg|_{(i\omega/c)\delta\mathbf{a}_{mac,\mathbf{q}=\mathbf{0}}=\hat{\mathbf{e}}}, \tag{70}$$

where the intraband contribution to the macroscopic conductivity tensor, $\sigma^{intra}(\mathbf{q},\omega)$, at $\mathbf{q}=\mathbf{0}$ is given by

$$\sigma^{intra}(\mathbf{q}=\mathbf{0},\omega) = \frac{-i}{\omega V}\int\int [\chi^{intra}_{\mathbf{jjq}=\mathbf{0}}(\mathbf{r},\mathbf{r}',\omega) - \chi^{intra,0}_{\mathbf{jjq}=\mathbf{0}}(\mathbf{r},\mathbf{r}',\omega=0)]\,d\mathbf{r}d\mathbf{r}'. \tag{71}$$

We can then consider the following expression for the macroscopic dielectric function at $q=0$,

$$\epsilon(\omega) = [1 + 4\pi\chi_e^{inter}(\omega)] - \frac{4\pi i}{\omega}\sigma^{intra}(\omega), \tag{72}$$

where the contribution in brackets is defined as the interband part of the dielectric function.

F. The energy loss function

In transmission electron energy loss spectroscopy one studies the inelastic scattering of a beam of high energy electrons by a target. The scattering rates obtained in these experiments are expressed in terms of the differential cross-section, which is obtained within the first Born approximation as[44]

$$\frac{d^2\sigma(\mathbf{k},\mathbf{k}',\omega)}{d\Omega d\omega} = \frac{2}{\pi q^4}\frac{k'}{k}S(\mathbf{q},\omega). \tag{73}$$

Here k and k' are the wave vectors of the incident and scattered electron, and $\mathbf{q}$ and ω are the transferred momentum and energy, respectively, with $\mathbf{q}=\mathbf{k}-\mathbf{k}'$ and $\omega=k^2/2-k'^2/2$. The dynamical structure factor $S(\mathbf{q},\omega)$ is related to the imaginary part of the true density-density response function via the fluctuation-dissipation theorem,

$$S(\mathbf{q},\omega) = -2\Im\int\int e^{-i\mathbf{q}\cdot(\mathbf{r}-\mathbf{r}')}\chi(\mathbf{r},\mathbf{r}',\omega)\,d\mathbf{r}d\mathbf{r}'. \tag{74}$$

Here the true density-density response function relates the induced density to an external perturbing scalar field,

$$\delta\rho(\mathbf{r},\omega) = \int \chi(\mathbf{r},\mathbf{r}',\omega)\delta v_{ext}(\mathbf{r}',\omega)\,d\mathbf{r}'. \tag{75}$$

If we choose the external perturbing field as $\delta v_{ext}(\mathbf{r},\omega) = e^{i\mathbf{q}\cdot\mathbf{r}}$, then the dynamical structure factor can be expressed as $S(\mathbf{q},\omega)=\Im\,\tilde{s}(\mathbf{q},\omega)$, where

$$\tilde{s}(\mathbf{q},\omega) = -2\int e^{-i\mathbf{q}\cdot\mathbf{r}}\delta\rho(\mathbf{r},\omega)\,d\mathbf{r}|_{\delta v_{ext}(\mathbf{r},\omega)=e^{i\mathbf{q}\cdot\mathbf{r}}} = -2\int \delta\rho_{\mathbf{q}}(\mathbf{r},\omega)\,d\mathbf{r}|_{\delta v_{ext,\mathbf{q}}=1}. \quad (76)$$

Here we used Eq. (14) for the induced density and the external potential. In our scheme we have to work in the microscopic Coulomb gauge and therefore we want to gauge transform the external macroscopic scalar potential to an external vector potential: we can have $i\omega\delta\mathbf{a}_{ext}(\mathbf{r},\omega)/c=\hat{\mathbf{q}}e^{i\mathbf{q}\cdot\mathbf{r}}$ if we choose the external scalar potential as $\delta v_{ext}(\mathbf{r},\omega)=(-i/q)e^{i\mathbf{q}\cdot\mathbf{r}}$. Then the same dynamical structure factor can be obtained using

$$\tilde{s}(\mathbf{q},\omega) = -2iq\int \delta\rho_{\mathbf{q}}(\mathbf{r},\omega)\,d\mathbf{r}|_{(i\omega/c)\delta a_{ext,\mathbf{q}}=\hat{\mathbf{q}}}. \quad (77)$$

Unlike in the case of the macroscopic dielectric function, here we need to consider the response to a given external field. Assuming Eq. (56) to hold, i.e., neglecting the sample-shape dependence of the induced field, the total macroscopic field can be related to the given external field according to

$$\frac{i\omega}{c}\delta\mathbf{a}_{mac,\mathbf{q}}(\mathbf{r},\omega) = \hat{\mathbf{q}}\left(1+\frac{4\pi i}{qV}\int \delta\rho_{\mathbf{q}}(\mathbf{r},\omega)\,d\mathbf{r}\right) = \hat{\mathbf{q}}\left(1-\frac{2\pi}{q^2V}\tilde{s}(\mathbf{q},\omega)\right). \quad (78)$$

In a completely similar way as for the calculation of the macroscopic dielectric function, we can now solve the SCF equations for a fixed macroscopic field and calculate the induced macroscopic density as linear response to this field,

$$\frac{i}{2q^2V}\tilde{s}(\mathbf{q},\omega) = \frac{1}{V}\int\frac{\delta\rho_{\mathbf{q}}(\mathbf{r},\omega)}{q}\,d\mathbf{r} = \frac{i\omega}{c}\int \mathbf{F}_{\mathbf{q}}(\mathbf{r},\omega)\cdot\delta\mathbf{a}_{mac,\mathbf{q}}(\mathbf{r},\omega)\,d\mathbf{r}. \quad (79)$$

By solving the SCF equations we obtain the lattice periodic response function $\mathbf{F}_{\mathbf{q}}(\mathbf{r},\omega)$. In the previous section we showed that for a finite macroscopic field the central term in the equation above is finite for vanishing q, and therefore also the terms on the left- and right-hand sides will be finite. By inserting Eq. (78) in Eq. (79) we can now account for the relation between the macroscopic and external fields to arrive at

$$\frac{i}{2q^2V}\tilde{s}(\mathbf{q},\omega) = \int \mathbf{F}_{\mathbf{q}}(\mathbf{r},\omega)\cdot\hat{\mathbf{q}}\left(1+4\pi i\frac{i}{2q^2V}\tilde{s}(\mathbf{q},\omega)\right)d\mathbf{r}, \quad (80)$$

from which we immediately obtain

$$\frac{i}{2q^2V}\tilde{s}(\mathbf{q},\omega) = \frac{\int \mathbf{F}_{\mathbf{q}}(\mathbf{r},\omega)\cdot\hat{\mathbf{q}}\,d\mathbf{r}}{1-4\pi i\int \mathbf{F}_{\mathbf{q}}(\mathbf{r},\omega)\cdot\hat{\mathbf{q}}\,d\mathbf{r}}. \quad (81)$$

Using now the definitions of the dynamical structure factor $S(\mathbf{q},\omega)$ and the response function $\mathbf{F}_{\mathbf{q}}(\mathbf{r},\omega)$, we can write

$$S(\mathbf{q},\omega) = -2q^2V\Re\left\{\frac{\frac{1}{V}\int\frac{\delta\rho_{\mathbf{q}}(\mathbf{r},\omega)}{q}\,d\mathbf{r}}{1-4\pi i\frac{1}{V}\int\frac{\delta\rho_{\mathbf{q}}(\mathbf{r},\omega)}{q}\,d\mathbf{r}}\right\}\Bigg|_{(i\omega/c)\delta\mathbf{a}_{mac,\mathbf{q}}=\hat{\mathbf{q}}}. \quad (82)$$

We can now consider the special case $q=0$ and show that it is related to the current-current response function, and hence the macroscopic dielectric function. Using Eqs. (64) and (66) in Eqs. (39) and (40) one can easily show that the following relations hold,

$$\lim_{q\to0}\frac{1}{q}\int\chi^{inter}_{\rho\rho\mathbf{q}}(\mathbf{r},\mathbf{r}',\omega)\,d\mathbf{r} = \frac{\hat{\mathbf{q}}}{\omega}\cdot\int\chi^{inter}_{\mathbf{j}\rho\mathbf{q}=\mathbf{0}}(\mathbf{r},\mathbf{r}',\omega)\,d\mathbf{r},$$

$$\lim_{q\to0}\frac{1}{q}\int\chi^{inter}_{\rho\mathbf{j}q}(\mathbf{r},\mathbf{r}',\omega)\,d\mathbf{r} = \frac{\hat{\mathbf{q}}}{\omega}\cdot\int\left[\chi^{inter}_{\mathbf{jj}\mathbf{q}=\mathbf{0}}(\mathbf{r},\mathbf{r}',\omega) - \chi^{inter}_{\mathbf{jj}\mathbf{q}\to\mathbf{0}}(\mathbf{r},\mathbf{r}',\omega=0)\right]d\mathbf{r}. \quad (83)$$

Therefore using Eq. (38) we can write

$$\lim_{q\to0}\frac{1}{V}\int\frac{\delta\rho^{inter}_{\mathbf{q}}(\mathbf{r},\omega)}{q}\,d\mathbf{r} = \frac{\hat{\mathbf{q}}}{\omega}\cdot\frac{1}{V}\int\delta\mathbf{j}^{inter}_{\mathbf{q}=\mathbf{0}}(\mathbf{r},\omega)\,d\mathbf{r}. \quad (84)$$

A similar relation holds for the intraband contribution. Using again Eqs. (64) and (66), but now in Eqs. (46) and (47), and using in addition the following relation[43]

$$\epsilon_{i\mathbf{k}+\mathbf{q}}-\epsilon_{i\mathbf{k}} = \mathbf{q}\cdot\int\psi^*_{i\mathbf{k}}(\mathbf{r})\hat{\mathbf{j}}_{\mathbf{q}}\psi_{i\mathbf{k}+\mathbf{q}}(\mathbf{r})\,d\mathbf{r}+\mathcal{O}(q^2), \quad (85)$$

one finds

$$\lim_{q\to0}\frac{\omega^2}{q^2}\int\chi^{intra}_{\rho\rho\mathbf{q}}(\mathbf{r},\mathbf{r}',\omega)\,d\mathbf{r} = \lim_{q\to0}\frac{\omega}{q}\hat{\mathbf{q}}\cdot\int\chi^{intra}_{\mathbf{j}\rho\mathbf{q}=\mathbf{0}}(\mathbf{r},\mathbf{r}',\omega)\,d\mathbf{r},$$

$$\lim_{q\to0}\frac{\omega}{q}\int\chi^{intra}_{\rho\mathbf{j}\mathbf{q}}(\mathbf{r},\mathbf{r}',\omega)\,d\mathbf{r} = \hat{\mathbf{q}}\cdot\int\left[\chi^{intra}_{\mathbf{jj}\mathbf{q}=\mathbf{0}}(\mathbf{r},\mathbf{r}',\omega) - \chi^{intra}_{\mathbf{jj}\mathbf{q}\to\mathbf{0}}(\mathbf{r},\mathbf{r}',\omega=0)\right]d\mathbf{r}. \quad (86)$$

Therefore, using Eq. (45) we can write

$$\lim_{q\to 0}\frac{1}{V}\int\frac{\delta\rho_{\mathbf{q}}^{intra}(\mathbf{r},\omega)}{q}\,d\mathbf{r}=\frac{\hat{\mathbf{q}}}{\omega}\cdot\frac{1}{V}\int\delta\mathbf{j}_{\mathbf{q}=\mathbf{0}}^{intra}(\mathbf{r},\omega)\,d\mathbf{r}. \tag{87}$$

From Eqs. (84) and (87) the long-wavelength limit of Eq. (82) can be written as

$$\lim_{q\to 0}\frac{1}{2q^2V}S(\mathbf{q},\omega)=\Re\left(\frac{-i\hat{\mathbf{q}}\cdot\frac{-i}{\omega V}\int\delta\mathbf{j}_{\mathbf{q}=\mathbf{0}}(\mathbf{r},\omega)\,d\mathbf{r}}{1+4\pi\hat{\mathbf{q}}\cdot\frac{-i}{\omega V}\int\delta\mathbf{j}_{\mathbf{q}=\mathbf{0}}(\mathbf{r},\omega)\,d\mathbf{r}}\right)\Bigg|_{(i\omega/c)\delta\mathbf{a}_{mac,\mathbf{q}}=\hat{\mathbf{q}}}. \tag{88}$$

Using the results of the previous section, Eqs. (69)–(72), we arrive at the final result

$$\lim_{q\to 0}\frac{2\pi}{q^2V}S(\mathbf{q},\omega)=\Im\left(\frac{-1}{\hat{\mathbf{q}}\cdot\boldsymbol{\epsilon}(\omega)\cdot\hat{\mathbf{q}}}\right). \tag{89}$$

The dynamical structure factor for all q and ω as given in Eq. (82) includes all the local field effects and can be used for both isotropic and anisotropic systems. In particular, in the limit of vanishing q the dynamical structure factor is directly related to the macroscopic dielectric function according to the relation given above.

III. IMPLEMENTATION

In this section we describe the main new aspects of the implementation for the dielectric function calculation in metallic systems. For the interband part we closely follow the implementation for nonmetallic crystalline systems described in Ref. 12. The main difference here is in the numerical evaluation of the **k**-space integrals. The response integrals of the set of equations (39)–(42) involve integrations over the (irreducible wedge of the) Brillouin zone, in which the denominator can become singular. These singularities have been treated, as described in Ref. 12, using a Lehmann-Taut tetrahedron scheme.[45] With partially occupied bands the numerical evaluation of integrals over tetrahedra in which the first Brillouin zone is partitioned is restricted to a part cut off by the Fermi surface. Both the energy and the integrand at the new corners of the truncated simplices are obtained by linear interpolation within each tetrahedron. The intraband contribution to the dielectric function is completely defined by Eq. (71). Inserting Eqs. (49) and (52) and replacing the summation over the **k**-points by an integral over the Brillouin zone $1/N_k\Sigma_{\mathbf{k}}\to V/8\pi^3\int d\mathbf{k}$, we arrive at

$$\sigma^{intra}(\omega)=\lim_{q\to 0}\left(\frac{-i}{8\pi^3\omega}\sum_i\int d\mathbf{k}\frac{df}{d\epsilon}\frac{\omega^2}{q^2(\boldsymbol{\nabla}_{\mathbf{k}}\boldsymbol{\epsilon}_{i\mathbf{k}}\cdot\hat{\mathbf{q}})^2-(\omega+i\eta)^2}\times\langle\psi_{i\mathbf{k}}^*|\hat{\mathbf{j}}_{\mathbf{q}}|\psi_{i\mathbf{k}+\mathbf{q}}\rangle\otimes\langle\psi_{i\mathbf{k}+\mathbf{q}}^*|\hat{\mathbf{j}}'_{-\mathbf{q}}|\psi_{i\mathbf{k}}\rangle\right). \tag{90}$$

The integration will be reduced to an integral over the sheets S_i of the Fermi surface originating by the bands i, as the first derivative of the Fermi-Dirac distribution $f(\epsilon)=2\Theta(\epsilon_F-\epsilon)$ peaks at $\epsilon=\epsilon_F$, $df/d\epsilon=-2\delta(\epsilon_F-\epsilon)$. For the frequency-dependent factor we can use the Cauchy theorem and write

$$\frac{\omega^2}{(\boldsymbol{\nabla}_{\mathbf{k}}\boldsymbol{\epsilon}_{i\mathbf{k}}\cdot\mathbf{q})^2-(\omega+i\eta)^2}=\mathcal{P}\frac{(\omega/q)^2}{(\boldsymbol{\nabla}_{\mathbf{k}}\boldsymbol{\epsilon}_{i\mathbf{k}}\cdot\hat{\mathbf{q}})^2-(\omega/q)^2}+i\pi(\omega/q)^2[\delta(\boldsymbol{\nabla}_{\mathbf{k}}\boldsymbol{\epsilon}_{i\mathbf{k}}\cdot\hat{\mathbf{q}}-\omega/q)+\delta(\boldsymbol{\nabla}_{\mathbf{k}}\boldsymbol{\epsilon}_{i\mathbf{k}}\cdot\hat{\mathbf{q}}+\omega/q)]. \tag{91}$$

In optical experiments ω/q is of the order of the velocity of light, $\omega/q\sim c$, which is much higher than the velocity in the direction of $\hat{\mathbf{q}}$ of valence electrons at the Fermi surface, $\nabla_{\mathbf{k}}\boldsymbol{\epsilon}_{i\mathbf{k}}\cdot\hat{\mathbf{q}}$. Thus, the imaginary part in Eq. (91) is zero and the real part reduces to -1 in the limit of $q\to 0$. In other experiments, where ω/q is of the same order as the Fermi velocity, the imaginary part can become important. In this case the integrations in the **k**-space are reduced to integrations over closed loops resulting from the intersection of the Fermi surface with a surface of constant velocity $(=\omega/q)$ parallel to **q**. Using the principal value of Eq. (91) in the optical limit, Eq. (90) becomes

$$\sigma^{intra}(\omega)=\frac{-i}{4\pi^3\omega}\sum_i\int_{S_i}\frac{d^2\mathbf{k}}{|\nabla_{\mathbf{k}}\boldsymbol{\epsilon}_{i\mathbf{k}}|}\langle\psi_{i\mathbf{k}}^*|\hat{\mathbf{j}}|\psi_{i\mathbf{k}}\rangle\otimes\langle\psi_{i\mathbf{k}}^*|\hat{\mathbf{j}}|\psi_{i\mathbf{k}}\rangle. \tag{92}$$

The integrations over the Fermi surface are evaluated numerically following the linear tetrahedron method proposed by Wiesenekker and Baerends.[46]

IV. RESULTS AND DISCUSSION

To test our method we calculated the optical dielectric functions $\boldsymbol{\epsilon}(\omega)$ in the spectral range 0–10 eV and the energy loss functions $-\Im[\boldsymbol{\epsilon}_L^{-1}(\omega)]$ in the spectral range 0–40 eV for the isotropic crystals of copper and silver within the adiabatic local density approximation. Both metals have the fcc lattice type for which we used the experimental lattice constants, 3.61 Å for Cu and 4.09 Å for Ag. All calculations were performed using a modified version of the ADF-BAND program.[12,13,47–49] We made use of a hybrid valence basis set consisting of Slater-type orbitals (STOs) in combination with the numerical solutions of a free-atom Herman-Skillman program.[50] Cores were kept frozen up to $3p$ and $4p$ for Cu and Ag, respectively. The spatial resolution of this basis is equivalent to a STO triple-zeta basis set augmented with two polarization functions. The Herman-Skillman program also provides us with the free-atom effective potential. The crystal potential was evaluated using an auxiliary basis set of STO functions to fit the deformation density in the ground-state calculation and the induced density in the response calculation. For the evaluation of the **k**-space integrals we used a quadratic numerical integration scheme with 175 symmetry-unique sample points in the irreducible wedge of the Brillouin zone, which was constructed by adopting a Lehmann-Taut tetrahedron scheme.[45,46] We found that the convergency and accuracy are very similar to the previous

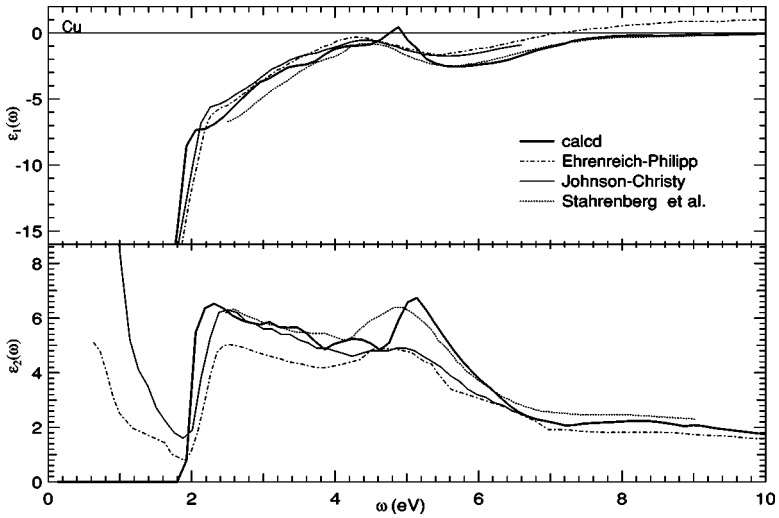

FIG. 5. Real (upper graph) and imaginary (lower graph) parts of the dielectric function of Cu. The bold solid line shows our calculation, the others show the experimental data from Refs. 35–37.

formulation for nonmetals and we checked that our results were converged with respect to **k**-space sampling and basis set size. All results shown here were obtained using the Vosko-Wilk-Nusair parametrization[51] of the LDA exchange-correlation potential, which was also used to derive the ALDA exchange-correlation kernel. In Figs. 5 and 6 the calculated real and imaginary parts of the dielectric functions of Cu and Ag are compared with two sets of experimental data well known in literature,[35,36] and with more recent measurements.[37] The latter data have been obtained using ultrahigh vacuum spectroscopic ellipsometry, thus we consider them the best data available. Our results are in good overall agreement with the experiments. In particular, the onset of the interband transitions at ~1.9 eV (experimentally around 2.0 eV) for Cu as well as the overall shape of ϵ_2 are very well reproduced by our calculations. For Ag the onset at ~3.7 eV (experimentally around 4.0 eV) is slightly shifted to lower frequency, but again the main features of ϵ_2 are well described by our method, in line with the general observation in semiconductors where the absorption gap is underestimated in the LDA. A feature clearly missing in our calculated spectra is the low-frequency tail in the imaginary part of the dielectric function. In perfect crystals this contribution comes from the scattering that free-conduction electrons have with phonons and with other electrons.[52,53] These phenomena are not described by the ALDA, where a frequency-independent xc-kernel $f_{xc}(\mathbf{r},\mathbf{r}')$ is used. In general, electron correlation effects (beyond ALDA) will lead to a frequency-dependent kernel $f_{xc}(\mathbf{r},\mathbf{r}'',\omega)$ which will, in general, be long range.[11] The electron-phonon interaction requires the use of a multicomponent-density functional approach.[54] The phonon-mediated electron correlation effects are then described by an extra contribution to the $f_{xc}(\mathbf{r},\mathbf{r}',\omega)$ kernel. In particular the long-range frequency-dependent $f_{xc}(\mathbf{r},\mathbf{r}',\omega)$ can take the form of a local functional of the current-density, which can be included in our scheme.[11,55] At the moment the use of such a frequency-dependent kernel is the subject of our ongoing research. The separation of the inter- and intraband contributions to the dielectric function gives a deeper insight in the linear response of the two metals, in particular in the role of bound and conduction electrons and in the identification of the plasma resonances. Plasmon excitations can be identified by the characteristic maxima in the energy loss function (EELS) occurring at energies where both ϵ_1 and ϵ_2 are small. In the measured dielectric functions of Refs. 35 and 36 the Drude theory is used to estimate the free-electron

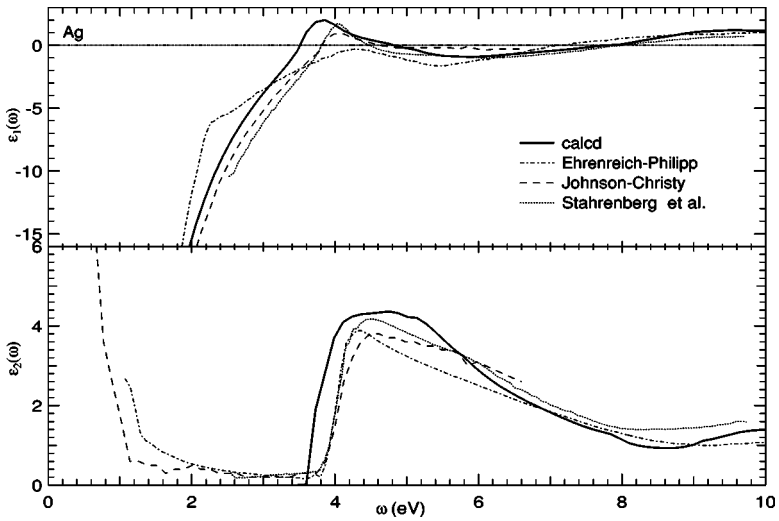

FIG. 6. Real (upper graph) and imaginary (lower graph) parts of the dielectric function of Ag. The bold solid line shows our calculation, the others show the experimental data from Refs. 35–37.

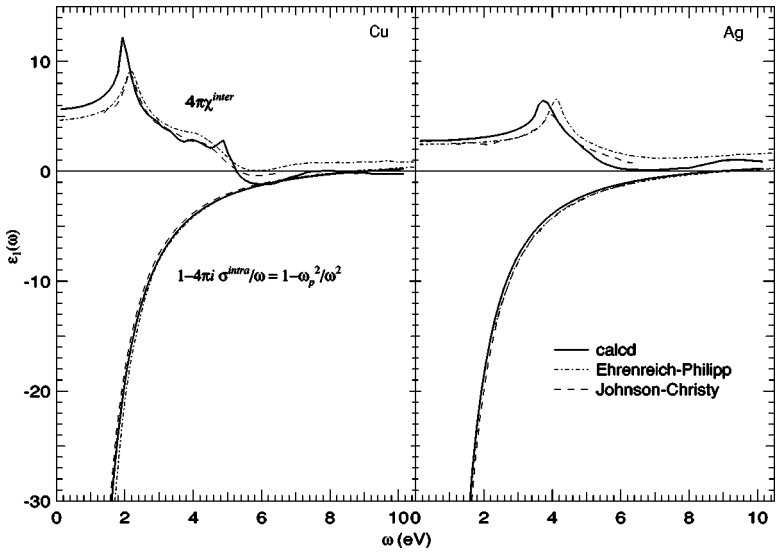

FIG. 7. The $4\pi\chi^{inter}$ and $1-4\pi i\sigma^{intra}/\omega$ contributions to the real part of the dielectric function of Cu (left) and Ag (right). Included are the decompositions of the experimental data using the Drude model as reported in Refs. 35 and 36.

contribution (intraband contribution). Within this model both the real and imaginary parts of the dielectric function in the free-electron region depend on the relaxation time τ and the plasma frequency ω_p,

$$\epsilon_1^D(\omega) = 1 - \frac{\omega_p^2\tau^2}{1+\omega^2\tau^2}, \tag{93}$$

$$\epsilon_2^D(\omega) = \frac{\omega_p^2\tau}{\omega(1+\omega^2\tau^2)}. \tag{94}$$

Here $\omega_p^2 = 4\pi N/m^*$ with N the density of conduction electrons and m^* their effective optical mass. In order to compare with our theory within the ALDA approach we have to consider the expressions (93) and (94) in the limit of τ to infinity. In this case, indeed, they become

$$\epsilon_1^D(\omega) = 1 - \frac{\omega_p^2}{\omega^2}, \tag{95}$$

$$\epsilon_2^D(\omega) = 0. \tag{96}$$

In our treatment the intraband contribution to ϵ_2 is zero, whereas Eqs. (72) and (92) show that for isotropic systems the intraband contribution to ϵ_1 can be written as

$$-\frac{4\pi i}{\omega}\sigma^{intra}(\omega) = -\frac{1}{3\pi^2\omega^2}\mathrm{Tr}\sum_i \int_{S_i} \frac{d^2\mathbf{k}}{|\nabla_{\mathbf{k}}\epsilon_{i\mathbf{k}}|}(\nabla_{\mathbf{k}}\epsilon_{i\mathbf{k}})\otimes(\nabla_{\mathbf{k}}\epsilon_{i\mathbf{k}})$$
$$= -\frac{1}{3\pi^2\omega^2}\sum_i \int_{S_i} d^2\mathbf{k}\nabla_{\mathbf{k}}\epsilon_{i\mathbf{k}}\cdot\hat{n}, \tag{97}$$

where the gradient $\nabla_{\mathbf{k}}\epsilon_{i\mathbf{k}} = |\nabla_{\mathbf{k}}\epsilon_{i\mathbf{k}}|\cdot\hat{n}$ is a vector normal to the Fermi surface. The integrals over the Fermi surface can be written as an integral over the occupied part of the Brillouin zone, thus we arrive at

$$-\frac{4\pi i}{\omega}\sigma^{intra}(\omega) = -\frac{1}{6\pi^2\omega^2}\sum_i \int_{BZ} d\mathbf{k} f_{i\mathbf{k}}\nabla_{\mathbf{k}}^2\epsilon_{i\mathbf{k}}. \tag{98}$$

Since the isotropic average effective mass m^* of the conduction electrons can be defined via $N/m^* = (8\pi^3)^{-1}\Sigma_i\int_{BZ} d\mathbf{k} f_{i\mathbf{k}}(\nabla_{\mathbf{k}}^2\epsilon_{i\mathbf{k}}/3)$, where N is the density of the conduction electrons $N=(8\pi^3)^{-1}\Sigma_i\int_{BZ} d\mathbf{k} f_{i\mathbf{k}}$, we can write Eq. (99) as

$$-\frac{4\pi i}{\omega}\sigma^{intra}(\omega) = -\frac{1}{\omega^2}\frac{4\pi N}{m^*} = -\left(\frac{\omega_p}{\omega}\right)^2, \tag{99}$$

with indeed $\omega_p^2 = 4\pi N/m^*$. In order to compare our results with those obtained using the Drude model, we plotted $4\pi\chi^{inter}$ and $1-4\pi i\sigma^{intra}/\omega$ separately in Fig. 7, together with the decomposition of the experimental data proposed in Refs. 35 and 36. We cannot compare with the data of Ref. 37, however, because the few values of the dielectric functions recorded at frequencies lower than the onset of the interband transitions makes it difficult to obtain the parameters τ and ω_p by fitting the experimental data. In Fig. 8 we report the energy loss spectra for both metals in the range 0–40 eV. Here calculated and experimental data[35,56] are compared. For both metals the calculated Drude-like part of the dielectric function crosses zero at frequencies around 8.9 and 8.8 eV, in good agreement with the free-electron plasma frequencies 9.3 eV for Cu and 9.2 eV for Ag found in Ref. 35. In copper this is the only resonance observed and it has to be interpreted as a free-electron like resonance.[35,38] However, in silver ϵ_1 crosses zero three times, at frequencies 3.5, 4.8, and 7.8 eV close to the experimental values. Sharp energy loss peaks are experimentally observed near the first and third frequencies.[35,37,39] The peak near the third frequency is a free-electron-like resonance as it is close to the Drude plasma frequency. Although ϵ_1 becomes zero twice near the onset of the interband transitions, only one peak appears in the EELS spectrum at a frequency near 3.8 eV where ϵ_2 is still small. Whereas the third resonance is well reproduced in the calculated spectrum, the first one is less intense than the one observed experimentally. Similar results

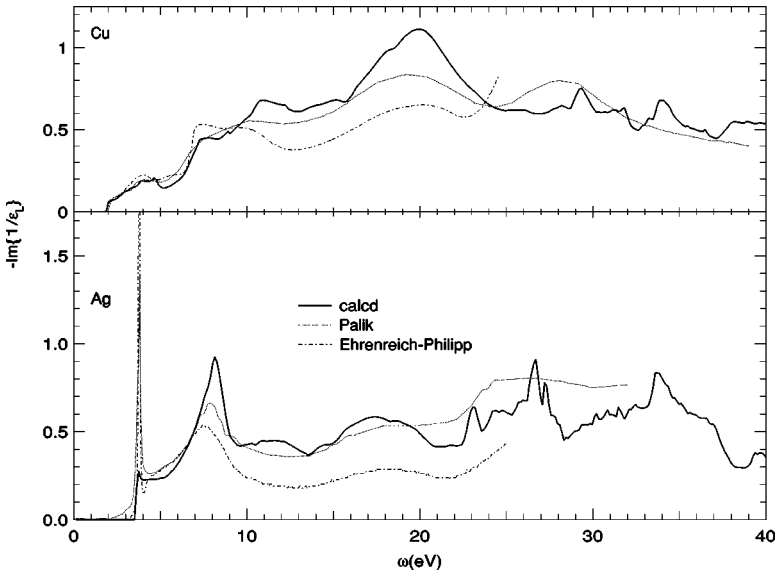

FIG. 8. The energy loss function of Cu (upper graph) and Ag (lower graph). The bold solid line shows our calculation, the others show the experimental data from Refs. 35 and 36.

have been found by Cazalilla *et al.*[39] In order for the first peak to gain intensity it is necessary to have a small but nonvanishing imaginary part of the dielectric function at the frequency where the real part crosses the zero axes. As becomes clear from Fig. 7, in silver this crossing occurs where the inter- and intraband contributions compensate, which is always below the peak appearing in the interband contribution to the real part of the dielectric function corresponding to the absorption onset. In copper the situation is different as here this compensation will occur in a region around 4.8 eV where the absorption is already strong. Unlike Cazalilla *et al.*[39] we expect that the use of more advanced approximations to the xc-functional in the ground state, although changing the band structure, will not affect the peak intensity in the case of silver. Instead inclusion of relaxation effects through the xc-kernel $f_{xc}(\mathbf{r},\mathbf{r}',\omega)$ is expected to strongly influence this peak. This is in keeping with the observation that the absorption is sensitive to the introduction of nonintrinsic sources of scattering.[57,58]

V. CONCLUSIONS

We have successfully extended the existing time-dependent current-density-functional approach originally developed for the calculation of the dielectric response of nonmetallic crystalline systems[12,13] to treat metallic systems. We describe the linear response of a metallic system to a general q- and ω-dependent external electromagnetic field and arrive at closed expressions for the $q=0$ limit at finite ω. We show how the macroscopic dielectric function and the energy loss function can be derived as a function of $\mathbf{q}$ and ω in our scheme. Three steps are essential in this procedure. First we show how the inter- and intraband contributions to the induced density and current-density can be separated. Then the microscopic Coulomb gauge is used. In this gauge the effective scalar potential is completely microscopic and all macroscopic contributions due to the inter- and intraband parts of the induced density and current-density are gauge transformed to the effective vector potential. Finally, we consider the limit of vanishing q. Since the macroscopic inter- and intraband parts of the induced density as well as the microscopic intraband part vanish in the optical limit, they cannot lead to exchange-correlation contributions unless there is a long-range part in the exchange-correlation functional. Using the local exchange-correlation functional, there is only a contribution to the exchange-correlation scalar potential due to the microscopic interband part of the induced density. From the last step we conclude that, within the ALDA and at $q=0$, the self-consistent-field equations describing the inter- and intraband contributions to the response decouple. In general, however, for $q>0$ and when going beyond the ALDA, inter- and intraband processes are interconnected. We have applied our approach to calculate the dielectric function and the energy loss function for Cu and Ag. Comparison of the ALDA results with experimental data shows a good overall agreement. Even though the onset for the interband transitions is shifted to lower frequency for both metals by about 10%, the main features of the spectra are well reproduced above the onset. Within the ALDA no relaxation processes are included which results in the absence of the Drude-like absorption tail below the interband onset. For both metals we obtain a macroscopic dielectric function, with $|\epsilon|\approx 0$, near the experimentally observed Drude-like free electron plasma frequencies. In silver, in addition, a vanishing dielectric function is observed at 3.5 eV, just below the interband absorption edge, and close to the experimental plasma resonance. This is not a free-electron resonance but the results of the combined response due to inter- and intraband processes. In our calculated loss spectrum the intensity of this plasmon peak is strongly underestimated, which cannot be attributed to the local density approximation for the xc-potential of the ground state but is the result of the absence of relaxation processes in our ALDA description.

APPENDIX: SYMMETRY OF THE RESPONSE FUNCTIONS

We consider a crystalline system perturbed by a potential $\delta\hat{\mathbf{h}}(\mathbf{r},\omega)$ with a periodicity that is consistent with the Born–

von Kármán boundary condition. Using linear response theory and the following transformation for the perturbation, $\delta\hat{\mathbf{h}}(\mathbf{r}'+\mathbf{R},\omega)=e^{i\mathbf{q}\cdot\mathbf{R}}\delta\hat{\mathbf{h}}(\mathbf{r},\omega)$, the first-order change in the density is given by

$$\delta\rho(\mathbf{r},\omega)=e^{i\mathbf{q}\cdot\mathbf{r}}\delta\rho_{\mathbf{q}}(\mathbf{r},\omega), \tag{A1}$$

in which the lattice periodic $\delta\rho_{\mathbf{q}}(\mathbf{r}+\mathbf{R},\omega)=\delta\rho_{\mathbf{q}}(\mathbf{r},\omega)$ is given by

$$\delta\rho_{\mathbf{q}}(\mathbf{r},\omega)=\frac{1}{N_k}\sum_{\mathbf{k},\mathbf{k}'}\sum_{n,n'}\delta_{\mathbf{k}',\mathbf{k}+\mathbf{q}}(f_{n\mathbf{k}}-f_{n'\mathbf{k}'})\times\frac{\psi^*_{n\mathbf{k}}(\mathbf{r})e^{-i\mathbf{q}\cdot\mathbf{r}}\psi_{n'\mathbf{k}'}(\mathbf{r})\langle\psi_{n'\mathbf{k}'}|\delta\hat{h}(\mathbf{q},\omega)|\psi_{n\mathbf{k}}\rangle}{\epsilon_{n\mathbf{k}}-\epsilon_{n'\mathbf{k}'}+\omega+i\eta}. \tag{A2}$$

In the following we will use the perturbation given in Eq. (16) and consider the time-reversal symmetry. Since only combinations of (partially) occupied, i, and (partially) unoccupied, a, orbitals contribute, we can write

$$\begin{aligned}\delta\rho_{\mathbf{q}}(\mathbf{r},\omega)=&\frac{1}{N_k}\sum_{\mathbf{k},\mathbf{k}'}\delta_{\mathbf{k}',\mathbf{k}+\mathbf{q}}\sum_{i,a}\frac{(f_{i\mathbf{k}}-f_{a\mathbf{k}'})}{1+\delta_{ia}}\times\frac{\psi^*_{i\mathbf{k}}(\mathbf{r})e^{-i\mathbf{q}\cdot\mathbf{r}}\psi_{a\mathbf{k}'}(\mathbf{r})\langle\psi_{a\mathbf{k}'}|\delta\hat{h}(\mathbf{q},\omega)|\psi_{i\mathbf{k}}\rangle}{\epsilon_{i\mathbf{k}}-\epsilon_{a\mathbf{k}'}+\omega+i\eta}\\&+\frac{1}{N_k}\sum_{\mathbf{k},\mathbf{k}'}\delta_{\mathbf{k}',\mathbf{k}-\mathbf{q}}\sum_{i,a}\frac{(f_{a\mathbf{k}'}-f_{i\mathbf{k}})}{1+\delta_{ia}}\times\frac{\psi^*_{a\mathbf{k}'}(\mathbf{r})e^{-i\mathbf{q}\cdot\mathbf{r}}\psi_{i\mathbf{k}}(\mathbf{r})\langle\psi_{i\mathbf{k}}|\delta\hat{h}(\mathbf{q},\omega)|\psi_{a\mathbf{k}'}\rangle}{\epsilon_{a\mathbf{k}'}-\epsilon_{i\mathbf{k}}+\omega+i\eta}.\end{aligned} \tag{A3}$$

In the second line we interchanged the role of $\mathbf{k}$ and $\mathbf{k}'$ and used that $\delta_{\mathbf{k},\mathbf{k}'+\mathbf{q}}=\delta_{\mathbf{k}',\mathbf{k}-\mathbf{q}}$. Furthermore, we introduced the factor $1/(1+\delta_{ia})$ to correct for the double counting of the diagonal terms with $i=a$. Introducing the time-reversed partners of $\psi_{i\mathbf{k}}$ and $\psi_{a\mathbf{k}'}$, namely $\psi^*_{i\mathbf{k}}=\psi_{i-\mathbf{k}}$ and $\psi^*_{a\mathbf{k}'}=\psi_{a-\mathbf{k}'}$, for which $\epsilon_{i\mathbf{k}}=\epsilon_{i-\mathbf{k}}$, $\epsilon_{a\mathbf{k}'}=\epsilon_{a-\mathbf{k}'}$, and $f_{i\mathbf{k}}=f(\epsilon_{i\mathbf{k}})=f(\epsilon_{i-\mathbf{k}})=f_{i-\mathbf{k}}$, etc.,[43] we can write

$$\begin{aligned}\delta\rho_{\mathbf{q}}(\mathbf{r},\omega)=&\frac{1}{N_k}\sum_{\mathbf{k},\mathbf{k}'}\delta_{\mathbf{k}',\mathbf{k}+\mathbf{q}}\sum_{i,a}\frac{(f_{i\mathbf{k}}-f_{a\mathbf{k}'})}{2(1+\delta_{ia})}\frac{\psi^*_{i\mathbf{k}}(\mathbf{r})e^{-i\mathbf{q}\cdot\mathbf{r}}\psi_{a\mathbf{k}'}(\mathbf{r})\langle\psi_{a\mathbf{k}'}|\delta\hat{h}(\mathbf{q},\omega)|\psi_{i\mathbf{k}}\rangle}{\epsilon_{i\mathbf{k}}-\epsilon_{a\mathbf{k}'}+\omega+i\eta}\\&+\frac{1}{N_k}\sum_{\mathbf{k},\mathbf{k}'}\delta_{\mathbf{k}',\mathbf{k}+\mathbf{q}}\sum_{i,a}\frac{(f_{i-\mathbf{k}}-f_{a-\mathbf{k}'})}{2(1+\delta_{ia})}\frac{\psi_{i-\mathbf{k}}(\mathbf{r})e^{-i\mathbf{q}\cdot\mathbf{r}}\psi^*_{a-\mathbf{k}'}(\mathbf{r})\langle\psi^*_{a-\mathbf{k}'}|\delta\hat{h}(\mathbf{q},\omega)|\psi^*_{i-\mathbf{k}}\rangle}{\epsilon_{i-\mathbf{k}}-\epsilon_{a-\mathbf{k}'}+\omega+i\eta}\\&+\frac{1}{N_k}\sum_{\mathbf{k},\mathbf{k}'}\delta_{\mathbf{k}',\mathbf{k}-\mathbf{q}}\sum_{i,a}\frac{(f_{i\mathbf{k}}-f_{a\mathbf{k}'})}{2(1+\delta_{ia})}\frac{\psi^*_{a\mathbf{k}'}(\mathbf{r})e^{-i\mathbf{q}\cdot\mathbf{r}}\psi_{i\mathbf{k}}(\mathbf{r})\langle\psi_{i\mathbf{k}}|\delta\hat{h}(\mathbf{q},\omega)|\psi_{a\mathbf{k}'}\rangle}{\epsilon_{i\mathbf{k}}-\epsilon_{a\mathbf{k}'}-\omega-i\eta}\\&+\frac{1}{N_k}\sum_{\mathbf{k},\mathbf{k}'}\delta_{\mathbf{k}',\mathbf{k}-\mathbf{q}}\sum_{i,a}\frac{(f_{i-\mathbf{k}}-f_{a-\mathbf{k}'})}{2(1+\delta_{ia})}\frac{\psi_{a-\mathbf{k}'}(\mathbf{r})e^{-i\mathbf{q}\cdot\mathbf{r}}\psi^*_{i-\mathbf{k}}(\mathbf{r})\langle\psi^*_{i-\mathbf{k}}|\delta\hat{h}(\mathbf{q},\omega)|\psi^*_{a-\mathbf{k}'}\rangle}{\epsilon_{i-\mathbf{k}}-\epsilon_{a-\mathbf{k}'}-\omega-i\eta}.\end{aligned} \tag{A4}$$

After a change of variables from $-\mathbf{k}$ and $-\mathbf{k}'$ to $\mathbf{k}$ and $\mathbf{k}'$ in the second and fourth terms we can gather the factors $(\psi^*_{i\mathbf{k}}e^{-i\mathbf{q}\cdot\mathbf{r}}\psi_{a\mathbf{k}'})$ from the first and fourth terms and the factor $(\psi^*_{a\mathbf{k}'}e^{-i\mathbf{q}\cdot\mathbf{r}}\psi_{i\mathbf{k}})$ from the second and third. Now, using the relations

$$\begin{aligned}\langle\psi^*_{i\mathbf{k}}|\delta\hat{h}(\mathbf{q},\omega)|\psi^*_{a\mathbf{k}'}\rangle&=\langle\psi_{i\mathbf{k}}|\delta\hat{h}^*(\mathbf{q},\omega)|\psi_{a\mathbf{k}'}\rangle^*\\&=\langle\psi_{a\mathbf{k}'}|(\delta\hat{h}^*(\mathbf{q},\omega))^\dagger|\psi_{i\mathbf{k}}\rangle\\&=\langle\psi_{a\mathbf{k}'}|\delta\hat{h}^*(-\mathbf{q},-\omega)|\psi_{i\mathbf{k}}\rangle,\end{aligned} \tag{A5}$$

in which $\delta\hat{h}(\mathbf{q},\omega)=\delta\hat{h}^\dagger(-\mathbf{q},-\omega)$, and reorganizing the terms a little, we arrive at Eq. (18). In a fully analogous way, but now taking into account the following relations,

$$\psi^*_{i\mathbf{k}}\hat{\mathbf{j}}\psi_{a\mathbf{k}'}=-\psi_{a\mathbf{k}'}\hat{\mathbf{j}}\psi^*_{i\mathbf{k}}=(\psi^*_{a\mathbf{k}'}\hat{\mathbf{j}}\psi_{i\mathbf{k}})^*=-(\psi_{i\mathbf{k}}\hat{\mathbf{j}}\psi^*_{a\mathbf{k}'})^*, \tag{A6}$$

we arrive at the response functions for the paramagnetic part of the induced current-density, Eq. (28).

*Electronic address: p.l.de.boeij@rug.nl

[1] E. Runge and E. K. U. Gross, Phys. Rev. Lett. **52**, 997 (1984).
[2] P. Hohenberg and W. Kohn, Phys. Rev. **136**, B864 (1964).
[3] W. Kohn and L. J. Sham, Phys. Rev. **140**, A1133 (1965).
[4] E. K. U. Gross and W. Kohn, Adv. Quantum Chem. **21**, 255 (1990).
[5] E. K. U. Gross, J. F. Dobson, and M. Petersilka, Top. Curr. Chem. **181**, 81 (1996).
[6] R. van Leeuwen, Int. J. Mod. Phys. B **15**, 997 (2001).
[7] A. K. Dhara and S. K. Ghosh, Phys. Rev. A **35**, 442 (1987).
[8] S. K. Ghosh and A. K. Dhara, Phys. Rev. A **38**, 1149 (1988).
[9] R. van Leeuwen, in *Progress in Nonequilibrium Green's Functions II*, edited by M. Bonitz and D. Semkat (World Scientific, New Jersey, 2003), p. 427.
[10] O.-J. Wacker, R. Kümmel, and E. K. U. Gross, Phys. Rev. Lett. **73**, 2915 (1994).
[11] G. Vignale and W. Kohn, Phys. Rev. Lett. **77**, 2037 (1996).
[12] F. Kootstra, P. L. de Boeij, and J. G. Snijders, J. Chem. Phys. **112**, 6517 (2000).
[13] F. Kootstra, P. L. de Boeij, and J. G. Snijders, Phys. Rev. B **62**, 7071 (2000).
[14] R. Resta, Rev. Mod. Phys. **66**, 899 (1994).
[15] X. Gonze, P. Ghosez, and R. W. Godby, Phys. Rev. Lett. **74**, 4035 (1995); **78**, 294 (1997).
[16] G. F. Bertsch, J. I. Iwata, A. Rubio, and K. Yabana, Phys. Rev. B **62**, 7998 (2000).
[17] P. Nozières and D. Pines, *The Theory of Quantum Liquids* (Perseus Books, Cambridge, MA, 1999).
[18] S. L. Adler, Phys. Rev. **126**, 413 (1962).
[19] N. Wiser, Phys. Rev. **129**, 62 (1963).
[20] G. Onida, L. Reining, and A. Rubio, Rev. Mod. Phys. **74**, 601 (2002).
[21] R. O. Jones and O. Gunnarson, Rev. Mod. Phys. **61**, 689 (1989).
[22] Z. H. Levine and D. C. Allan, Phys. Rev. B **43**, 4187 (1991); **44**, 12781 (1991); Phys. Rev. Lett. **66**, 41 (1991).
[23] M. S. Hybertsen and S. G. Louie, Phys. Rev. B **34**, 5390 (1986).
[24] R. W. Godby, M. Schlüter, and L. J. Sham, Phys. Rev. Lett. **56**, 2415 (1986); Phys. Rev. B **37**, 10159 (1988).
[25] J. Chen, Z. H. Levine, and J. W. Wilkins, Phys. Rev. B **50**, 11514 (1994).
[26] V. I. Gavrilenko and F. Bechstedt, Phys. Rev. B **54**, 13416 (1996).
[27] L. Reining, V. Olevano, A. Rubio, and G. Onida, Phys. Rev. Lett. **88**, 066404 (2002).
[28] Y.-H. Kim and A. Görling, Phys. Rev. B **66**, 035114 (2002); Phys. Rev. Lett. **89**, 096402 (2002).
[29] F. Sottile, V. Olevano, and L. Reining, Phys. Rev. Lett. **91**, 056402 (2003).
[30] R. Del Sole, G. Adragna, V. Olevano, and L. Reining, Phys. Rev. B **67**, 045207 (2003).
[31] A. Marini, R. Del Sole, and A. Rubio, Phys. Rev. Lett. **91**, 256402 (2003).
[32] I. V. Tokatly, R. Stubner, and O. Pankratov, Phys. Rev. B **65**, 113107 (2002).
[33] G. Vignale and W. Kohn, in *Electronic Density Functional Theory: Recent Progress and New Directions*, edited by J. Dobson *et al.* (Plenum Press, New York, 1998).
[34] P. L. de Boeij, F. Kootstra, J. A. Berger, R. van Leeuwen, and J. G. Snijders, J. Chem. Phys. **115**, 1995 (2001).
[35] H. Ehrenreich and H. R. Philipp, Phys. Rev. **128**, 1622 (1962).
[36] P. B. Johnson and R. W. Christy, Phys. Rev. B **6**, 4370 (1972).
[37] K. Stahrenberg, Th. Herrmann, K. Wilmers, N. Esser, and W. Richter, Phys. Rev. B **64**, 115111 (2001).
[38] I. Campillo, A. Rubio, and J. M. Pitarke, Phys. Rev. B **59**, 12188 (1999).
[39] M. A. Cazalilla, J. S. Dolado, A. Rubio, and P. M. Eschenique, Phys. Rev. B **61**, 8033 (2000).
[40] G. Breit, Phys. Rev. **34**, 553 (1929); **39**, 616 (1932).
[41] O. L. Brill and B. Goodman, Am. J. Phys. **35**, 832 (1967).
[42] T. Kjeldaas and W. Kohn, Phys. Rev. **105**, 806 (1957).
[43] M. Lax, *Symmetry Principles in Solid State and Molecular Physics* (Dover Publications, Mineola, NY, 2001).
[44] S. E. Schnatterly, in *Solid State Physics Vol. 34* edited by H. Ehrenreich, F. Seitz, and D. Turnbull (Academic Press, New York, 1979).
[45] G. Lehmann and M. Taut, Phys. Status Solidi B **54**, 469 (1972).
[46] G. Wiesenekker, and E. J. Baerends, J. Phys.: Condens. Matter **3**, 6721 (1991); G. Wiesenekker, G. te Velde, and E. J. Baerends, J. Phys. C **21**, 4263 (1988).
[47] G. te Velde and E. J. Baerends, Phys. Rev. B **44**, 7888 (1991); J. Comput. Phys. **99**, 84 (1992).
[48] C. Fonseca Guerra, O. Visser, J. G. Snijders, G. te Velde, and E. J. Baerends, in *Methods and Techniques in Computational Chemistry*, edited by E. Clementi and G. Corongiu (STEF, Cagliari, 1995), p. 305.
[49] G. te Velde, F. M. Bickelhaupt, E. J. Baerends, C. Fonseca Guerra, S. J. A. van Gisbergen, J. G. Snijders, and T. Ziegler, J. Comput. Chem. **22**, 931 (2001).
[50] F. Herman and S. Skillman, *Atomic Structure Calculations* (Prentice-Hall, Englewood Cliffs, NJ, 1963).
[51] S. H. Vosko, L. Wilk, and M. Nusair, Can. J. Phys. **58**, 1200 (1980).
[52] R. T. Beach and R. W. Christy, Phys. Rev. B **16**, 5277 (1977).
[53] G. R. Parkins, W. E. Lawrence, and R. W. Christy, Phys. Rev. B **23**, 6408 (1981).
[54] R. van Leeuwen, Phys. Rev. B **69**, 115110 (2004).
[55] J. A. Berger, P. L. de Boeij, and R. van Leeuwen, Phys. Rev. B (to be published).
[56] E. D. Palik, *Handbook of Optical Constants of Solids* (Acaademic Press, New York, 1985).
[57] R. M. Morgan and D. W. Lynch, Phys. Rev. **172**, 628 (1968).
[58] G. B. Irani, T. Huen, and F. Wooten, Phys. Rev. B **3**, 2385 (1971).